ELSEVIER

Journal of Nuclear Materials 288 (2001) 100–129

journal of nuclear materials

www.elsevier.nl/locate/jnucmat

Thermodynamic modelling of the C–U and B–U binary systems

P.Y. Chevalier *, E. Fischer

Thermodata, INPG-CNRS, UMS THERMA, BP 66, F-38402, Saint Martin d'Hères cedex, France

Received 19 June 2000; accepted 7 November 2000

Abstract

The thermodynamic modelling of the carbon–uranium (C–U) and boron–uranium (B–U) binary systems is being performed in the framework of the development of a thermodynamic database for nuclear materials, for increasing the basic knowledge of key phenomena which may occur in the event of a severe accident in a nuclear power plant. Applications are foreseen in the nuclear safety field to the physico-chemical interaction modelling, on the one hand the in-vessel core degradation producing the corium (fuel, zircaloy, steel, control rods) and on the other hand the ex-vessel molten corium–concrete interaction (MCCI). The key O–U–Zr ternary system, previously modelled, allows us to describe the first interaction of the fuel with zircaloy cladding. Then, the three binary systems Fe–U, Cr–U and Ni–U were modelled as a preliminary work for modelling the O–U–Zr–Fe–Cr–Ni multicomponent system, allowing us to introduce the steel components in the corium. In the existing database (TDBCR, thermodynamic data base for corium), Ag and In were introduced for modelling AIC (silver–indium–cadmium) control rods which are used in French pressurized water reactors (PWR). Elsewhere, B_4C is also used for control rods. That is why it was agreed to extend in the next years the database with two new components, B and C. Such a work needs the thermodynamic modelling of all the binary and pseudo-binary sub-systems resulting from the combination of B, B_2O_3 and C with the major components of TDBCR, O–U–Zr–Fe–Cr–Ni–Ag–In–Ba–La–Ru–Sr–Al–Ca–Mg–Si + Ar–H. The critical assessment of the very numerous experimental information available for the C–U and B–U binary systems was performed by using a classical optimization procedure and the Scientific Group Thermodata Europe (SGTE). New optimized Gibbs energy parameters are given, and comparisons between calculated and experimental equilibrium phase diagrams or thermodynamic properties are presented. The self-consistency obtained is quite satisfactory.

1. Introduction

Since 1989, THERMODATA and IPSN (Institut de Protection et de Sûreté Nucléaire, CEA France) have been working at the development of a thermodynamic database for corium and concrete materials (TDBCR) in the framework of the nuclear reactor safety.

Corium is a partially molten complex mixture, resulting from the degradation of the core and its thermochemical interaction with the other materials present in a nuclear reactor in the unlikely event of a severe accident. If the corium goes through the vessel and slumps into the concrete reactor cavity, the phenomenon is called molten corium–concrete interaction (MCCI).

The selected major components of TDBCR, [O–U–Zr–Fe–Cr–Ni–Ag–In–Ba–La–Ru–Sr–Al–Ca–Mg–Si] + [Ar–H] were deduced from the inventory of the materials present in a pressurized water reactor (PWR): fuel (UO_2), zircaloy (Zr), steel structures (Fe, Cr, Ni), control rods AIC (Ag, In, Cd), selected fission products (Ba, La, Ru, Sr), concrete (Al_2O_3, CaO, FeO, Fe_2O_3, MgO, SiO_2), water (H_2O) and air.

The thermodynamic modelling of such a complex multicomponent system is based on the critical assessment of the most important binary and higher-order sub-systems (metallic, oxide, metal-oxide/oxygen) from

* Corresponding author.

0022-3115/01/$ - see front matter
PII: S0022-3115(00)00713-3

all the available experimental information (phase diagram and thermodynamics).

The global thermodynamic approach of the MCCI and selected applications in the nuclear field was previously presented in a general view by Chevalier et al. [1].

The thermodynamic modelling of the key ternary metal–oxygen O–U–Zr system, including the O–U, O–Zr, U–Zr and UO_2–ZrO_2 sub-systems, was first undertaken by Chevalier and Fischer [2] and recently reviewed by Chevalier et al. [3]. It allows us to study the first core degradation, i.e. the interaction of the fuel rods with the metallic zircaloy at high temperature.

Then, the critical assessment of the three binary systems Fe–U, Cr–U and Ni–U by using an appropriate optimization procedure was presented by Chevalier and Fischer [4] as a preliminary work for the thermodynamic modelling of the multicomponent system O–U–Zr–Fe–Cr–Ni. This second step was needed to introduce chrome and nickel steel in the corium.

In the actual database, Ag and In were introduced for modelling AIC (Ag, In, Cd) control rods which are used in French PWR. However, B_4C is also commonly used. For this reason, the extension of the nuclear thermodynamic database with two new components, B and C, will be undertaken in the next three years. Such a work needs the thermodynamic modelling of all the binary and pseudo-binary sub-systems resulting from the combination of B, B_2O_3 and C with the other major components of TDBCR.

The critical assessment of the very numerous experimental information available for the carbon–uranium (C–U) and boron–uranium (B–U) binary systems was here performed by using a classical optimization procedure and the 'Scientific Group Thermodata Europe' (SGTE) standards (models and lattice-stabilities of pure elements) [5,6].

The coefficients of the Gibbs energy versus temperature for stoichiometric substances, and of the excess Gibbs energy versus temperature and composition for solutions, were optimized by using the optimization programme developed by Lukas et al. [7], which allows us to take into account simultaneously all the available experimental information.

In this work, we present for each binary system, C–U and B–U, the existing equilibrium phases, the analysis of the compiled experimental data, concerning both phase diagram and thermodynamic properties, and the optimization results: on the one hand, optimized Gibbs energy parameters of all condensed substance and solution phases are given; on the other hand, phase diagrams and specific thermodynamic properties are calculated and compared to the experimental ones.

Practical applications of the extended nuclear thermodynamic database (NTD) are expected both for in-vessel and ex-vessel phenomena, for example calculations of corium properties (phase diagram – liquidus, solidus, ..., viscosity, ...), fission products release in the atmosphere, and finally coupling the global thermodynamic approach with more general thermohydraulics nuclear safety codes.

2. The C–U system

2.1. Short presentation of the different phases

The phase diagram of the C–U binary system was successively reported in a compilation work by Hansen and Anderko [8], Elliott [9], Shunk [10], Hultgren et al. [11] (similar to the one compiled by Storms [12] and Massalski [13]). Another entire phase diagram was reported in the experimental work of Benz et al. [14]. The C–U phase diagrams taken from Storms [12] and Benz et al. [14] are presented in Figs. 1 and 2, respectively.

The condensed solutions and stoichiometric substances, with the symbols currently used in this work, are as follows: liquid phase, L; (UC, UC_2), intermediate solid solution, fcc_B1 or δ, isotypic with NaCl; separates below 2373 K in: (UC), UC-rich solid solution and (UC_2) or β-UC_2, UC_2-rich solid solution, high-temperature form; U_2C_3 or ε, bcc (D5c) structure, isotypic with Pu_2C_3, $C_3U_2(S)$; (UC_2) or α-UC_2-rich solid solution, low-temperature form, body-centred tetragonal (C11a) structure isotypic with CaC_2; pure uranium: U_1(ort_A20) or α-U; U_1(tet) or β-U; U_1(bcc_A2) or γ-U; pure carbon: C_1(gra_hex_A9) or C. No mutual solubility of carbon in uranium and uranium in carbon was reported.

The (UC, UC_2) solid solution (fcc_B1) presents two maximum melting points and a minimal melting point at high temperatures. At lower temperature, there is a

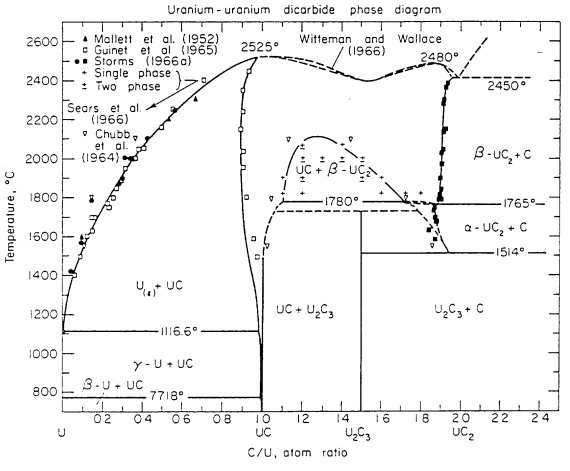

Fig 1. Phase diagram of the U–C system taken from Storms [12].

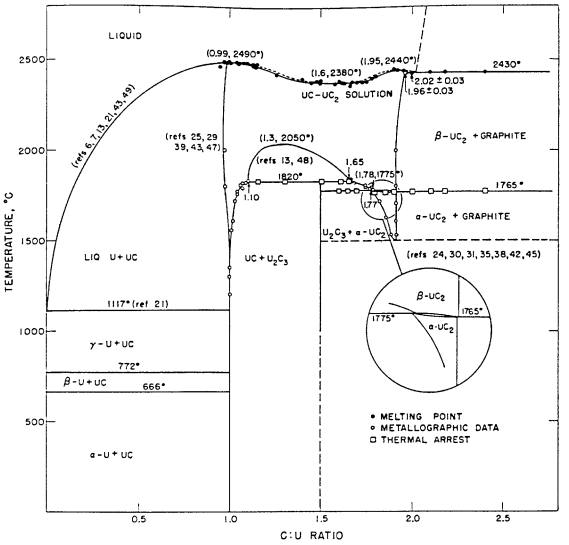

Fig. 2. Phase diagram of the U–C system taken from Benz et al. [14].

miscibility gap in the solid state between a (UC)-rich solid solution and a (UC_2)-rich solid solution.

The structures of the intermetallic compounds are given by Hansen and Anderko [8], Elliott [9] and Shunk [10] and reported in Table 1.

2.2. Experimental information

In the following, T is the temperature in Kelvin (Celsius are quoted between brackets), $x(\mathrm{U})$ or x is the uranium atomic fraction in one phase, x^{G} is the global uranium atomic fraction, L is the liquidus or the liquid and S is the solidus. In all tables, values between brackets are not experimental but estimated for the optimization.

2.2.1. Phase diagram

The following invariant reactions and transitions have been reported in the different compilations or experimental works and are summarized in Table 2.

Mallet et al. [30] investigated the entire system by using conventional experimental techniques (melting point, X-ray and metallographic data) and drew a constitutional phase diagram. Three uranium carbides, UC,

Table 1
Crystal characteristics of the stoichiometric compounds in the C–U system

Compound	Structure	Lattice parameter	Reference
UC	fcc_B1 type, isotypic with NaCl	$a = 4.961$ Å	[15]
		$a = 4.965$ Å	[16]
		$a = 4.9591 \pm 0.0002$ Å	[18]
		$a = 4.9598 \pm 0.0003$ Å	[19]
		$a = 4.9563 \pm 0.0007$ Å (48 a/o C)	[25]
		$a = 4.956$ Å*	[26]
		$a = 4.9577 \pm 0.0007$ Å*	[27]
		*(alloy sintered at 1673 K)	[25]
		$a = 4.9597 \pm 0.0004$ Å (stoichiometric UC)	[28]
UC_2	fcc_B1 type, isotypic with CaF_2	$a = 5.41$ Å	[21]
		$a = 5.45$ Å	[22]
		$a = 5.45 \pm 0.01$ Å	[23]
		$a = 5.475$ Å	[24]
η-UC_2	bc tetragonal, 2 molecules per unit cell, isotypic with CaC_2 (C11a)	$a = 3.524$ Å, $c = 5.999$ Å	[15]
		$a = 3.517 \pm 0.002$ Å, $c = 5.987 \pm 0.002$ Å	[20] [19]
		$a = 3.509 \pm 0.003$ Å, $c = 5.980 \pm 0.005$ Å	
		vary from $a = 3.5190 \pm 0.0011$ Å, $c = 5.9787 \pm 0.0017$ Å (U-rich) to $a = 3.5241 \pm 0.0005$ Å, $c = 5.9962 \pm 0.0008$ Å (C-rich)	[29]
U_2C_3	bcc, 8 molecules per unit cell	$a = 8.088$ Å	[17]
		$a = 8.089 \pm 0.0004$ Å	[29]

Table 2
Experimental and calculated three-phase equilibria and congruent transformations in the C–U system

Reaction	Experimental			Reference	Calculated		
	T (K)	t (°C)	x		T (K)	t (°C)	x
$L \Longleftrightarrow (UC)$	2833	2560	0.476	[10]			
	2798	2525	0.486	[11,12]			
	2763	2490	0.497	[14]	2788	2515	0.500
$LL \Longleftrightarrow (UC_2)$	2803	2530	0.370	[10]			
	2753	2480	0.360	[11,12]			
	2713	2440	0.339	[14]	2707	2435	0.345
$L \Longleftrightarrow (UC, UC_2)$	2623	2350	0.425	[9]			
	2673	2400	0.390	[11,12]			
	2723	2450	0.425	[10]	2676	2403	0.400
	2653	2380	0.385	[14]			
$L \Longleftrightarrow \gamma\text{-U} + (UC)$	1406	1133		[8]			
	1389.75	1116.6		[11,12]			
	1390	1117		[14]			
	1390	1117	0.9902^{L}	[9,10]	1390	1117	0.990^{L}
			$0.9882^{\gamma\text{-U}}$				
$L \Longleftrightarrow \gamma\text{-U}$	1408	1135		[6]	1408	1135	
$\gamma\text{-U} \Longleftrightarrow \beta\text{-U}$	1049	776		[6]	1049	776	
$\beta\text{-U} \Longleftrightarrow \alpha\text{-U}$	942	669		[6]	942	669	
$\gamma\text{-U} \Longleftrightarrow \beta\text{-U} + (UC)$	1043	770		[8]			
	1044.95	771.8		[12]			
	1045	772	$0.9991^{\gamma\text{-U}}$	[9,10]			
	1045	772		[14]			
	1048	775		[11]	1049	776	
$\beta\text{-U} \Longleftrightarrow \alpha\text{-U} + (UC)$	938	665		[8]			
	939	666		[9,10]			
	939	666		[14]	942	669	
$L \Longleftrightarrow (UC_2) + C$	2723	2450	$0.34^{\delta\text{-U}}$	[10]			
	2723	2450		[11,12]			
	2703	2430	$0.338^{\delta\text{-U}}$	[14]	2699	2426	$0.344^{\gamma\text{-U}}$
			0.331^{L}				0.330^{L}
$(UC_2) \Longleftrightarrow (UC) + \alpha\text{-}UC_2$	2073	1780		[9]	Not calculated		
$(UC) + (UC_2) \Longleftrightarrow \alpha\text{-}UC_2$	2053	1780		[11,12]	Not calculated		
$(UC) + (UC_2) \Longleftrightarrow \varepsilon\text{-}U_2C_3$	2153	1880		[10]			
	2093	1820	0.377^{UC_2}	[14]	2106	1833	0.387^{UC_2}
			0.476^{UC}				0.474^{UC}
$(UC_2) + C \Longleftrightarrow \alpha\text{-}UC_2$	2093	1820		[9,10]	Not calculated		
$(UC_2) \Longleftrightarrow \alpha\text{-}UC_2 + C$	2038	1765		[11,12]	2036	1763	0.344^{UC_2}
				[14]			$0.344^{\alpha\text{-}UC_2}$
$(UC_2) \Longleftrightarrow \varepsilon\text{-}U_2C_3 + \alpha\text{-}UC_2$	2073	1800		[10]	Not calculated		
$(UC) + \alpha\text{-}UC_2 \Longleftrightarrow \varepsilon\text{-}U_2C_3$	2048	1775		[8,9]	Not calculated		
	2000	1727		[11,12]			
$(UC_2) + \varepsilon\text{-}U_2C_3 \Longleftrightarrow \alpha\text{-}UC_2$	2048	1775	0.360^{UC_2}	[14]	2030	1757	0.357^{UC_2}
			$0.361^{\alpha\text{-}UC_2}$				$0.356^{\alpha\text{-}UC_2}$
$\alpha\text{-}UC_2 \Longleftrightarrow \varepsilon\text{-}U_2C_3 + C$	1773	1500		[10,14]	1751	1478	
	1787	1514		[11,12]			
$(UC, UC_2) \Longleftrightarrow (UC) + (UC_2)$	2323	2050	0.425	[10,14]	2323	2050	0.438
	2380	2107	0.445	[11,12]			

U_2C_3 and UC_2, were identified. UC and UC_2 are completely miscible at elevated temperature, forming a solid solution, and separate on cooling below 2323 K (2050°C). The reaction $\delta(UC) + \alpha\text{-}UC_2 \Longleftrightarrow \varepsilon\text{-}U_2C_3$ was located at about 2048 K (1775°C). The experimental results were reported by Hansen and Anderko [8]. The experimental liquidus and solidus points are reported from the original numerical values in Table 3, as the one-phase and two-phase (UC, UC_2) solid solution domains.

Blumenthal [31] studied the U-rich domain of the phase diagram by using saturation experiments, thermal analysis and metallography. The following invariant reactions were determined: the eutectic reaction $L \Longleftrightarrow \gamma\text{-}U + \delta$: $T = 1389.75$ K (1116.6°C), $x^{L}(U) = 0.9902$, $x^{\gamma\text{-}U}(U) = 0.9963 - 0.9978$g; the two eutectoid reactions $\gamma\text{-}U \Longleftrightarrow \beta\text{-}U + \delta$: $T = 1044.95$ K (771.8°C), $x^{\gamma\text{-}U}(U) = 0.9987$–$0.9995$ and $\beta\text{-}U \Longleftrightarrow \alpha\text{-}U + \delta$: $T = 939.05$ K (665.9°C). The uranium content in γ-U increased from $x = 0.9970 \pm 0.00075$ at 1389.75 K (1116.6°C) to $x = 0.9991 \pm 0.0004$ at 1044.95 K (771.8°C). The solubility of carbon was less than 10 ppm by weight in β-U and less than 3 ppm in α-U. These values have been reported by Elliott [9], Shunk [10], Hultgren et al. [11], Storms [12] and Benz et al. [14]. The experimental liquidus of Blumenthal [31] and the reported results of Carter [32] and Snow [33], taken from a figure in the original paper, are quoted in Table 4. The experimental liquidus points of Snow [33] were not in good agreement with those of Carter [32] and Blumenthal [31].

The melting point of (UC) was determined as 2663 K (2390°C) by Mallet et al. [30], 2863 ± 50 K (2590°C) by Chiotti [34] (values reported by Hansen and Anderko

Table 3
Liquidus, solidus and one-phase and two-phase (UC, UC_2) solid solution domains from Mallet et al. [30]

T^{L} (K)	t^{L} (°C)	$x^{\phi 1}(U)$	$x^{\phi 2}(U)$	Equilibrium
1873	1600	0.91276	(0.510)	$L(\phi 1) + \delta\text{-}UC(\phi 2)$
2273	2000	0.74023	(0.521)	–
2473	2200	0.65402	(0.522)	–
2573	2300	0.60188	(0.521)	–
2663	2390	0.49586	(0.517)	–
2668	2395	0.49264	(0.517)	–
2723	2450	0.43675	(0.447)	$L(\phi 1) + \delta\text{-}(UC, UC_2)(\phi 2)$
2728	2455	0.41660	(0.427)	–
2733	2460	0.39408	(0.384)	–
2758	2485	0.38023	(0.370)	–
2758	2485	0.36283	(0.353)	–
2753	2480	0.33784	(0.345)	$L(\phi 1) + \delta\text{-}(UC_2)(\phi 2)$
2773	2500	0.32287	(0.345)	$L(\phi 1) + C(\phi 2)$
2873	2600	0.28991	(0)	–
2953	2680	0.28991	(0)	–
2973	2700	0.27010	(0)	–
T^{S} (K)	t^{S} (°C)	$x^{\phi 1}(U)$	$x^{\phi 2}(U)$	Equilibrium
2653	2380	0.43675	(0.427)	$\delta\text{-}(UC, UC_2)(\phi 1) + L(\phi 2)$
2683	2410	0.41660	(0.407)	–
2683	2410	0.39408	(0.404)	–
2663	2390	0.38023	(0.390)	–
2668	2415	0.36283	(0.373)	–
T (K)	t (°C)	$x^{G}(U)$		Equilibrium
2073	1800	0.41660		$\delta(UC) + \delta(UC_2)$
2173	1900	0.41660		$\delta(UC) + \delta(UC_2)$
2273	2000	0.41660		$\delta(UC) + \delta(UC_2)$
2373	2100	0.41660		$\delta(UC, UC_2)$
2073	1800	0.46921		$\delta(UC) + \delta(UC_2)$
2173	1900	0.46921		$\delta(UC) + \delta(UC_2)$
2273	2000	0.46921		$\delta(UC) + \delta(UC_2)$
2373	2100	0.46921		$\delta(UC, UC_2)$
2073	1800	0.49478		$\delta(UC) + \delta(UC_2)$
2173	1900	0.49478		$\delta(UC, UC_2)$
2273	2000	0.49478		$\delta(UC, UC_2)$
2373	2100	0.49478		$\delta(UC, UC_2)$

Table 4
U–C phase diagram at low-carbon content from Blumenthal [31], Carter [32] and Snow [33]

T^L (K)	t^L (°C)	$x^{\phi 1}$(U)	$x^{\phi 2}$(U)	Equilibrium	Reference
1623	1350	0.9753	(0.504)	L(ϕ1) + δ-UC(ϕ2)	[31]
1573	1300	0.9800	(0.503)	–	–
1523	1250	0.9833	(0.502)	–	–
1473	1200	0.9859	(0.502)	–	–
1389.76	1116.6	0.9902	(0.501)	L + δ-UC + γ	
1648	1375	0.9735	(0.504)	L(ϕ1) + δ-UC(ϕ2)	[32]
1673	1400	0.9670	(0.504)	–	–
1648 ± 50	1375	0.9806	(0.504)	–	[33]
1748 ± 50	1475	0.9675	(0.506)	–	–
T^S (K)	t^S (°C)	$x^{\phi 1}$(U)	$x^{\phi 2}$(U)	Equilibrium	Reference
1389.75	1116.6	0.99705 ± 0.0008	(0.501)	γ(ϕ1) + UC	[31]
1044.95	771.8	0.9991 ± 0.0004	(0.500)	γ + UC + β	–
1044.95	771.8	0.9998	(0.500)	β(ϕ1) + UC	–
939.09	665.9	0.99994	(0.500)	α(ϕ1) + UC + β	–

[8]), 2793 K (2520°C) by Brownlee [35], 2553 ± 50 K (2280°C) by Newkirk and Bates [36] (values reported by Elliott [9]), 2768 ± 30 K (2495°C) by Witteman et al. [37], 2833 ± 50 K (2560°C), $x = 0.476$ by Witteman and Bowman [29], and 2683 K (2410°C) by White et al. [38] (values reported by Shunk [10]). The values of Mallet et al. [30], Newkirk and Bates [36] and White et al. [38] are below the others. According to Witteman et al. [37], UC_2 in contact with C melts at 2723 ± 50 K (2450°C), value reported by Storms [12], Shunk [10] and Hultgren et al. [11].

Chubb and Phillips [39] studied the constitution of the partial system UC–UC_2 by using diffusion couples, metallography, optical pyrometry. The existence of a miscibility gap between (UC), with the NaCl-type crystal structure, and (UC_2), high-temperature form, with the CaF_2-type structure was put in evidence at 2473 K (2200°C), and supposed to be maintained up to an eutectic reaction, L $\Longleftrightarrow$ (UC) + (UC_2), located at 2623 K (2350°C). The immiscibility at high temperatures is in real contradiction with all the other experimental information summarized in the most recent compilation works [12,14]. An eutectoid reaction (β-UC_2) $\Longleftrightarrow$ (UC) + (α-UC_2) was located just below 2073 K (1800°C) (value reported by Elliott [9]). The transformation of cubic UC_2 to tetragonal UC_2 occurs at 2093 K (1820°C) by a peritectoïd-type reaction [9,10]. The temperature of the decomposition reaction δ(UC) + α-UC_2 $\Longleftrightarrow$ ε-U_2C_3 was reported as about 1973 K (1700°C) by Storms [12], 2048 K (1775°C) by Elliott [9], below 2060 K by Hultgren et al. [11], and 2093 K (1820°C) by Benz et al. [14].

The system UC–UC_2 was investigated at temperatures up to 2473 K (2200°C) by Wilson [40] using high-temperature X-ray diffraction technique. The transformation α-UC_2, which has the CaC_2 structure, to β-UC_2, with the CaF_2 structure, occurs at 2093 K (1820°C). The decomposition of U_2C_3 in δ(UC) + β-UC_2 occurs at 2113 ± 20 K (1840°C), a value near the one of Benz et al. [14] (2093 K). Solubilities of UC in UC_2 and UC_2 in UC were determined near 2073 K (1800°C). Experimental results are reported in Table 5 from the original figure.

According to Chang [21], a diffusionless phase transformation between the high-temperature UC_2 phase (CaF_2) to a tetragonal structure (CaC_2) takes place at 2093 K (1820°C) to 2103 K (1830°C). We can underline here that the CaF_2-type structure of the

Table 5
UC–UC_2 phase diagram reported from Wilson [40]

T (K)	t (°C)	w (%C)	$x^{\phi 1}$(U)	$x^{\phi 1}$(U)	Equilibrium
1969	1696	5	0.48947	0.4	δ-UC(ϕ1) + U_2C_3(ϕ2)
2058	1785	5.13	0.48271	0.4	–
2079	1806	5.20	0.47915	0.4	–
2093	1820	5.31	0.47364	0.4	δ-UC(ϕ1) + U_2C_3(ϕ2) + δ-UC_2
1969	1696	8.96	0.33894	0.4	α-UC_2(ϕ1) + U_2C_3(ϕ2)
2093	1820	8.65	0.34764	0.4	–
2132	1859	5.31	0.47364	(0.35)	δ-UC(ϕ1) + δ-UC_2(ϕ2)
2163	1890	5.54	0.46247	(0.36)	–

high-temperature form of (UC_2), proposed by Chubb and Phillips [39], Wilson [40] and Chang [21], is definitively incompatible with a complete miscibility of the solid solution (UC, UC_2) at high temperature, this one having a NaCl-type structure.

Guinet et al. [41] determined in the system U–UC, the liquidus by the saturation method, the solidus by equilibrating the liquid and the solid phases and the eutectic temperature on the uranium side by differential thermal analysis. Experimental results are reported in Table 6 from the original figure.

Sears et al. [42] studied the high-temperature immiscibility of uranium mono and dicarbides by microstructure examinations. Specimens with compositions from $UC_{1.1}$ to $UC_{1.8}$ were prepared by decomposing mixtures containing uranium sesquicarbide at temperatures from 2093 to 2403 K (1820–2130°C). The low-carbon immiscibility boundary is nearly composition invariant between 2093 K (1820°C) and 2343 K (2070°C) and occurs between $UC_{1.1}$ and $UC_{1.2}$ ($0.454 < x < 0.476$). The high-carbon immiscibility boundary occurs at about $UC_{1.65}$ ($x = 0.377$) at 2093 K (1820° C) and the solubility of the monocarbide in the dicarbide phase increases linearly with increasing temperature. The peak of the immiscible region occurs at about $UC_{1.3}$ ($x = 0.435$) and a temperature around 2373 K (2100°C). Experimental results are reported in Table 7 from the original figure.

In the phase diagram presented by Storms [12] in its compilation work (Fig. 1), the phase boundary between β/α-UC_2 and C, in the temperature range 1873–2723 K

Table 6
Liquidus and solidus of the U–UC phase diagram from Guinet et al. [41]

T^L (K)	t^L (°C)	$x^{\phi 1}$(U)	$x^{\phi 2}$(U)	Equilibrium
U + UC Liquidus				$L(\phi 1) + \delta\text{-UC}(\phi 2)$
1673	1400	0.94479	(0.504)	–
1773	1500	0.91829	(0.505)	–
1873	1600	0.89013	(0.511)	–
1903	1630	0.86430	(0.511)	–
1973	1700	0.85038	(0.514)	–
1973	1700	0.84315	(0.514)	–
2037	1764	0.81858	(0.516)	–
2044	2771	0.82335	(0.517)	–
2073	1800	0.80313	(0.517)	–
2123	1850	0.78779	(0.520)	–
2159	1886	0.77168	(0.519)	–
2223	1950	0.76326	(0.522)	–
2273	2000	0.74012	(0.524)	–
2323	2050	0.72457	(0.522)	–
2323	2050	0.71203	(0.522)	–
2437	2164	0.66814	(0.524)	–
2523	2250	0.63464	(0.524)	–
2673	2400	0.57973	(0.522)	–
2723	2450	0.56328	(0.518)	–
T^S (K)	t^S (°C)	$x^{\phi 1}$(U)	$x^{\phi 2}$(U)	Equilibrium
U + UC Solidus				$UC(\phi 1) + L(\phi 2)$
1673	1400	0.50411	(0.945)	–
1773	1500	0.50544	(0.918)	–
1873	1600	0.51073	(0.890)	–
2073	1800	0.51682	(0.803)	–
2223	1950	0.52168	(0.763)	–
2323	2050	0.52168	(0.725)	–
2323	2050	0.52168	(0.712)	–
2423	2150	0.52450	(0.668)	–
2523	2250	0.52450	(0.635)	–
2623	2350	0.52310	(0.604)	–
2723	2450	0.51752	(0.563)	–
T (K)	t (°C)	$x^{\phi 1}$(U)	$x^{\phi 2}$(U)	Equilibrium
1390.15 ± 2	1117	0.98847	(0.500)	$L(\phi 1) + \delta\text{-UC}(\phi 2) + \gamma\text{-U}$

Table 7
High-temperature immiscibility of uranium mono and dicarbides from Sears et al. [42]

T (K)	t (°C)	$x^{G}(U)$		Equilibrium
2093 ± 20	1820	0.47619		$\delta(UC)$
2093	1820	0.45455		$\delta(UC) + \delta(UC_2)$
2093	1820	0.38314		$\delta(UC) + \delta(UC_2)$
2093	1820	0.36590		$\delta(UC_2)$
2093	1820	0.35714		$\delta(UC_2)$
2173	1900	0.47619		$\delta(UC)$
2173	1900	0.45455		$\delta(UC) + \delta(UC_2)$
2173	1900	0.40161		$\delta(UC) + \delta(UC_2)$
2173	1900	0.38314		$\delta(UC_2)$
2273	2000	0.45455		$\delta(UC) + \delta(UC_2)$
2273	2000	0.43478		$\delta(UC) + \delta(UC_2)$
2273	2000	0.41667		$\delta(UC) + \delta(UC_2)$
2273	2000	0.40000		$\delta(UC_2)$
2343	2070	0.45455		$\delta(UC) + \delta(UC_2)$
2343	2070	0.44307		$\delta(UC) + \delta(UC_2)$
2343	2070	0.41667		$\delta(UC_2)$
2403	2130	0.43478		$\delta(UC_2)$
2403	2130	0.36900		$\delta(UC_2)$
T (K)	t (°C)	$x^{\phi 1}(U)$	$x^{\phi 2}(U)$	Equilibrium
2093	1820	(0.383)	(0.472)	$(UC) + \delta(UC_2)$
2173	1900	(0.390)	(0.469)	–
2273	2000	(0.408)	(0.463)	–
2343	2070	(0.424)	(0.459)	–

Table 8
δ/α-UC_2 + C phase boundary from Storms [12]

t (°C)	T (K)	$C/U^{\phi 1}$	$x^{\phi 1}(U)$	$x^{\phi 2}(U)$	Equilibrium
1873	1603	1.874	0.348	1	α-$UC_2(\phi 1)$ + C
1918	1645	1.842	0.352	–	–
1958	1685	1.884	0.347	–	–
1978	1705	1.879	0.347	–	–
2018	1745	1.863	0.349	–	–
2033	1760	1.874	0.348	–	–
2073	1800	1.900	0.345	–	δ-$UC_2(\phi 1)$ + C
2088	1815	1.900	0.345	–	–
2113	1840	1.905	0.344	–	–
2173	1900	1.900	0.345	–	–
2243	1970	1.910	0.344	–	–
2303	2030	1.910	0.344	–	–
2328	2055	1.916	0.343	–	–
2413	2140	1.921	0.342	–	–
2433	2160	1.932	0.341	–	–
2553	2280	1.921	0.342	–	–
2573	2300	1.923	0.342	–	–
2633	2360	1.932	0.341	–	–
2353	2380	1.937	0.340	–	–

(1600–2450°C), is reported from an original paper of the author. Experimental results are reported in Table 8 from the original figure.

The entire U–C phase diagram presented by Benz et al. [14] (Fig. 2) gathers the literature results and own investigations. The experimental results were obtained by using conventional techniques (thermal, microscopic, X-ray diffraction and chemical analyses). The three-phase equilibria and congruent transformations are reported in Table 2. Experimental results are reported in Table 9 from original numerical and graphical results. The accuracy of the melting temperatures was given as 40 K, while that of the U_2C_3 decomposition and the allotropic transformation of UC_2 was given as 25 K.

Table 9
U–C phase diagram and some other values reported from Benz et al. [14]

T (K)	t (°C)	$C/U^{\phi 1}$	$x^{\phi 1}(U)$	$x^{\phi 2}(U)$	Equilibrium	Reference
1473	1200	1	0.50000	0.4	δ-UC($\phi 1$) + U_2C_3($\phi 2$)	[14]
1573	1300	1	0.50000	0.4	–	–
1598	1325	1	0.50000	0.4	–	–
1833	1560	1.01	0.49751	0.4	–	–
1993	1720	1.03 ± 0.01	0.49261 ± 0.002	0.4	–	–
2025	1752	1.04	0.49020	0.4	–	–
2043	1770	1.04	0.49020	0.4	–	–
2078	1805	1.06	0.48544	0.4	–	–
2059	1786	1.07	0.48309	0.4	–	–
2077	1804	1.07 ± 0.02	0.48309 ± 0.005	0.4	–	–
2091	1818	1.09	0.47847	0.4	–	–
2093	1820	1.10	0.47619	0.4	δ-UC($\phi 1$) + U_2C_3($\phi 2$) + δ-UC_2	
1973	1700	1.21	0.45249	0.4	δ-UC($\phi 1$) + U_2C_3($\phi 2$)	[48]
2073	1800	1.24	0.44643	0.4	–	[49]
1773	1500	<1.08	<0.4808	0.4	–	[50]
2093	1820	1.1 to 1.2	0.46512 ± 0.01	0.4	–	[51]
2093	1820	1.10	0.47619	(0.377)	δ-UC($\phi 1$) + δ-UC_2($\phi 2$) + U_2C_3	–
2098	1825	1.10 ± 0.03	0.47619 ± 0.007	(0.377)	δ-UC($\phi 1$) + δ-UC_2($\phi 2$)	–
2103	1830	1.10	0.47619	(0.377)	–	–
2113	1840	1.11	0.47393	(0.376)	–	[40]
1793	1520	1.88 ± 0.03	0.34722	0.4	η-UC_2($\phi 1$) + U_2C_3($\phi 2$)	[14]
1891	1618	1.85	0.35088	0.4	–	–
1990	1717	1.82	0.35461	0.4	–	–
2001	1728	1.80	0.35714	0.4	–	–
2025	1752	1.79	0.35842	0.4	–	–
2028	1755	1.78	0.35971	0.4	–	–
2028	1755	1.78	0.35971	0.4	–	–
2035	1762	1.78	0.35971	0.4	–	–
2038	1765	1.78	0.35971	0.4	–	–
2038	1765	1.78	0.35971	0.4		–
1940	1667	1.78	0.35971	0.4	–	–
2044	1771	1.77	0.36101	0.4	–	–
2045	1772	1.77	0.36101	0.4	–	–
2048	1775	1.77	0.36101	0.4	η-UC_2($\phi 1$) + U_2C_3($\phi 2$) + δ-UC_2	–
2048	1775	1.78	0.35971	0.4	η-UC_2($\phi 1$) + U_2C_3($\phi 2$) + δ-UC_2	–
2051	1778	1.78	0.35971	0.4	δ-UC_2($\phi 1$) + U_2C_3($\phi 2$)	–
2051	1778	1.78	0.35971	0.4	–	–
2053	1780	1.77	0.36101	0.4	–	–
2054	1781	1.77	0.36101	0.4	–	–
2055	1782	1.76	0.36232	0.4	–	–
2062	1789	1.76	0.36232	0.4	–	–
2065	1792	1.74	0.36496	0.4	–	–
2077	1804	1.74	0.36496	0.4	–	–
2091	1818	1.68	0.37313	0.4	–	–
2098	1825	1.65	0.37736	0.476	δ-UC_2($\phi 1$) + δ-UC($\phi 2$)	–
2103	1830	1.65	0.37736	0.476	–	–
1773	1500	1.905	0.34423	0	η-UC_2($\phi 1$) + C_1-gra($\phi 2$) + U_2C_3	[14]
1793	1520	1.905 ± 0.02	0.34423	0	η-UC_2($\phi 1$) + C_1-gra($\phi 2$)	–
1873	1600	1.905	0.34423	0	–	–
1973	1700	1.905	0.34423	0	–	–
2038	1765	1.905	0.34423	0	η-UC_2($\phi 1$) + C_1-gra($\phi 2$) + δ-UC_2	–
2073	1800	1.905	0.34423	0	δ-UC_2($\phi 1$) + C_1-gra($\phi 2$)	–
2273	2000	1.915	0.34305	0	–	–

Table 9 (Continued)

T (K)	t (°C)	C/U$^{\phi 1}$	$x^{\phi 1}$(U)	$x^{\phi 2}$(U)	Equilibrium	Reference
2703	2430	1.96	0.33784	0	δ-$UC_2(\phi 1)$ + C_1-gra($\phi 2$) + L	–
2703	2430	2.02	0.33113	0	L($\phi 1$) + C1-gra($\phi 2$) + δ-UC_2	–
2073	1800	0.97 ± 0.02	0.50761	(0.8)	δ-UC($\phi 1$) + L	–
2273	2000	0.97 ± 0.02	0.50761	(0.8)	δ-UC($\phi 1$) + L	–
Liquidus/Solidus						
2743	2470	0.96	0.51020	(0.510)	L/δ-UC, UC_2	–
2763	2490	0.99	0.50251	(0.503)	–	–
2762	2489	1.00	0.50000	(0.500)	–	–
2755	2482	1.05	0.48780	(0.479)	–	–
2749	2476	1.10	0.47619	(0.476)	–	–
2738	2465	1.15	0.46512	(0.465)	–	–
2691	2418	1.25	0.44444	(0.444)	–	–
2668	2395	1.40	0.41666	(0.417)	–	–
2655	2380	1.45	0.40816	(0.408)	–	–
2655	2380	1.50	0.40000	(0.400)	–	–
2655	2380	1.60	0.38462	(0.385)	–	–
2655	2380	1.65	0.37736	(0.377)	–	–
2655	2380	1.70	0.37037	(0.370)	–	–
2668	2395	1.80	0.35714	(0.357)	–	–
2703	2430	1.90	0.34483	(0.345)	–	–
2713	2440	1.92	0.34247	(0.342)	–	–
2713	2440	1.95	0.33898	(0.339)	–	–

The phase boundaries of the miscibility gap in the (UC, UC_2) solid solution were determined by Tetenbaum and Hunt [43] from carbon activity measurements as: T (K), $x(UC_2)$, $x(UC) = 2155$, >0.377, 0.488; 2255, >0.377, 0.465; 2355, >0.385, 0.444.

The formation of U_2C_3 by the reaction of UC_2 with UO_2 was studied by chemical and X-ray analyses at temperatures between 1673 and 1973 K by Tagawa and Fujii [44]. The transformation of U_2C_3 phase in UC–UC_2 and UC_2 phases was characterized by Kurasawa et al. [45].

The stability of the UC_2-phase and its decomposition reaction $2UC_2 \Longleftrightarrow U_2C_3 + C$ was studied by Schneider et al. [46], with emphasis on the presence of certain moderating and accelerating forces.

Scherff and Springer [47] redetermined the equilibrium phase boundary between δ-UC and β-UC_2 in the temperature range 2173–2373 K (1900-2100°C), for C/U ranging from the stoichiometry up to the congruently vapourizing composition (1.00–1.08). Results are markedly different from earlier ones obtained on the basis of quenching experiments and the precipitation of β-UC_2 occurs at much lower C/U ratios than those assumed up to now. Experimental results are reported in Table 10 from numerical original values.

2.2.2. Thermodynamic properties

The heat and the entropy of formation the uranium carbides UC, U_3C_2 and $UC_{1.9-1.93}$ were reported by Hultgren et al. [11] as follows: $\Delta H°_{298.15\ K}(U_{0.5}C_{0.5})$ (J/g at.) = −45606 [52], −41422 [53], −34727 [54], −46861 [55], −35146 [56], −48534 [57], −48534 [12], -48534 ± 2092; $\Delta S°_{298.15\ K}$ $(U_{0.5}C_{0.5})$ (J/g at. K) = 1.925 ± 0.126 (selected by Hultgren et al. [11]). $\Delta H°_{298.15\ K}$ $(U_{0.4}C_{0.6})$ (J/g at.) = -41003 ± 3347; $\Delta S°_{298.15\ K}$ $(U_{0.4}C_{0.6})$ (J/g at. K) = 4.058 ± 0.126 (selected by Hultgren et al. [11]). $\Delta H°_{298.15\ K}(U_{0.34}C_{0.66})$ (J/g at.) = −31798 [58], −30962 [60], −27614 [61], −31380 [62], −31798 [63], −18410 [54], −30442 [64], −33890 [65], −31380 [57], −30125 [66], -30543 ± 2929; $\Delta S°_{298.15\ K}$ $(U_{0.34}C_{0.66})$ (J/g at. K) = 2.385 ± 0.126 (selected by Hultgren et al. [11]).

The heat of formation of the uranium monocarbide, UC, was measured by Farr et al. [52] by combustion calorimetry: $\Delta H°_{298.15\ K}(U_{0.5}C_{0.5}) = -43932 \pm 2092$ J/g at. The carbide was prepared by a direct combination of the elements, and the UC–UO_2 mixtures used in combustion experiments led to U_3O_8 as the final uranium oxide formed.

The thermodynamic properties of uranium dicarbide were investigated by Fujishiro [59] by measuring the dissociation pressure of uranium in the reaction $UC_2(S) = U(G) + 2C(S)$ using the Knudsen cell effusion method. The Gibbs energy of the reaction $0.333U(S) + 0.667C(S) \Longleftrightarrow U_{0.333}C_{0.667}(S)$ was estimated by combining the obtained results with other thermodynamic data to be $-46359 + 4.1924T$ J/g at. in the range 2448–2731 K.

The heat of formation of uranium dicarbide, $UC_{1.90}$, was determined indirectly by Huber et al. [64], from measurements of its heat of combustion in oxygen. The calculated values for three series of run were, respectively: $\Delta H°_{298.15\ K}(U_{0.345}C_{0.655}) = -28422 \pm 2885$,

Table 10
δ-UC/δ-UC + δ-UC_2 phase boundary from Scherff and Springer [47]

T (K)	t (°C)	$C/U^{\phi 1}$	$x^{\phi 1}(U)$	Equilibrium
2218 ± 5	1945	1.006	0.49850	δ-UC($\phi 1$) + δ-UC($\phi 2$)
2221 ± 4	1948	1.006	0.49850	–
2220 ± 3	1947	1.008	0.49801	–
2253 ± 20	1980	1.010	0.49751	–
2294 ± 4	2021	1.019	0.49529	–
2326 ± 5	2053	1.026	0.49358	–
2275 ± 2	2002	1.032	0.49212	–
2319 ± 5	2046	1.036	0.49116	–
2328 ± 2	2055	1.043	0.48948	–
2348 ± 20	2075	1.045	0.48900	–
2353 ± 10	2080	1.063	0.48473	–
2357 ± 10	2084	1.072	0.48263	–
2371 ± 12	2098	1.070	0.48309	–
2381 ± 12	2108	1.081	0.48054	–
2415 ± 10	2142	1.080	0.48077	–
2533 ± 13	2260	1.076	0.48170	–

$-26835 \pm 2813, -30442 \pm 2020$ J/g at. The third one was selected as the best (higher purity and combustion).

The heat content of uranium dicarbide and the specific heat of uranium dicarbide, S $UC_{1.93}$, were measured by Levinson [67] from 1484 to 2581 K, using a drop calorimeter. The experimental error was estimated as ±2%. The transition temperature from the low-temperature form (α or bct) to the high-temperature form (β or Sfcc_B1) was located at 2043 K (1770°C). Experimental results are reported in Table 11 from the original table.

The standard molar free energy of formation of uranium dicarbide, UC_2, and uranium sesquicarbide, U_2C_3, has been determined by Behl and Egan [66] by means of solid state galvanic cells operated between 973 and 1173 K.

Table 11
Experimental enthalpy of $UC_{1.93}$ versus temperature from Levinson [67]

T (K)	H_T–H_{310} (J/g at.)	C_p (J/g at. K)
1484	32750	33.943
1490	33205	33.943
1587	36208	36.181
1689	40284	38.419
1794	44425	40.657
1878	47894	42.523
2016	54086	45.880
2021	54086	45.880
2043	Tetragonal ⟺ Cubic	
2081	60427	37.300
2086	61285	37.673
2213	65723	39.911
2277	68223	41.403
2393	73668	43.642
2483	77249	45.134
2581	81837	47.372

$0.333U(tet) + 0.667C(S) \Longleftrightarrow U_{0.333}C_{0.667}(S)$:

$\Delta G = -22064 - 11.43627T$ J/g at.

$0.333U(bcc\_A2) + 0.667C(S) \Longleftrightarrow U_{0.333}C_{0.667}(S)$:

$\Delta G = -26471 - 7.25227T$ J/g at.

$0.400U(tet) + 0.600C(S) \Longleftrightarrow U_{0.400}C_{0.600}(S)$:

$\Delta G = -36702 - 5.8576T$ J/g at.

The heat transport properties (thermal conductivity) and heat capacity of monocarbide, monophosphide and monosulphite of uranium, UC, UP and US, were measured by Moser and Kruger [68] between room temperature and 873 K, by using a transient technique with a laser as a heat pulse source. Results are reported in Table 12 from the original table.

Thermodynamic properties of uranium carbides UC and $UC_{1.93}$ were analysed by Leitnaker and Godfrey [69] and shown to be consistent. Thermal functions were calculated and reported in Table 13 from the original table.

Table 12
Experimental enthalpy of UC versus temperature from Moser and Kruger [68]

T (K)	H_T–H_{298} (J/g at.)	C_p (J/g at. K)	S_T–S_{298} (J/g at. K)
400	2678	26.987	7.740
500	5439	28.242	13.807
600	8326	29.288	19.037
700	11297	30.125	23.640
800	14351	30.962	27.824
900	17489	31.798	31.589
1000	20711	32.426	34.936

Table 13
Thermal functions of $UC(U_{0.500}C_{0.500})$ and $UC_{1.93}(U_{0.341}C_{0.659})$ versus temperature from Leitnaker and Godfrey [69]

T (K)	$U_{0.500}C_{0.500}$			$U_{0.341}C_{0.659}$		
	C_p (J/g at. K)	H_T–H_{298} (J/g at.)	$S°_T$ (J/g at. K)	C_p (J/g at. K)	H_T–H_{298} (J/g at.)	$S°_T$ (J/g at. K)
298	25.33412	0	29.87376	20.80576	0	24.07585
300	25.39688	46	30.02020	20.86288	39	24.20437
400	27.36336	2699	37.63508	23.34758	2258	30.57319
500	28.38844	5489	43.86924	25.03260	4682	35.97098
600	29.05788	8364	48.86454	26.13215	7244	40.64049
700	29.60180	11299	53.63888	26.84614	9895	44.72453
800	30.08296	14282	57.61368	27.37450	12606	48..35162
900	30.56412	17315	61.19100	27.83145	15367	51.59315
1000	31.04528	20395	64.43360	28.37409	18177	54.56336
1100	31.54736	23522	67.40424	29.07380	21047	57.29081
1200	32.07036	26704	70.18660	30.00200	23999	59.86119
1300	32.61428	29939	72.75976	31.21578	27056	62.30304
1400	33.20004	33229	75.20740	32.70089	30250	64.67350
1500	33.82764	36581	77.50860	34.47159	33608	66.98684
1600	34.45524	39995	79.72612	36.48505	37153	69.27162
1700	35.14560	43474	81.83904	38.65559	40910	71.55640
1800	35.83596	47024	83.86828	40.91181	44889	73.82689
1900	36.58908	50645	85.81384	43.12519	49091	76.09739
2000	37.34220	54342	87.71756	45.13865	53507	78.36789
2060				46.18108	56247	79.71020
2060				36.97057	60175	81.62370
2100	38.13716	58114	89.55852	37.75596	61670	82.33769
2200	38.95304	61970	91.33672	39.72658	65545	84.13696
2300	39.81076	65908	93.09400	41.69720	69616	85.95050
2400	40.68940	69932	94.80944	43.66782	73883	87.76404
2500	41.58896	74046	96.48304	45.63844	78348	89.59186
2600	42.53036	78251	98.13572	47.59478	83009	91.41968
2700	43.47176	82550	99.76748	49.56541	87868	93.24751
2800	44.45500	86948	101.3574	51.53603	92923	95.08961
2900				53.50665	98175	96.93171
3000				55.47727	103625	98.77382

Craig et al. [70] measured the Gibbs free energies of formation of uranium monocarbide (1115–1165 K) and uranium dicarbide (1015–1160 K) by equilibrating two-phase mixtures of $UC_2 + C$ and $UC_2 + UC$ with liquid bismuth. The uranium activities in these two-phase regions were deduced from the measured equilibrium concentrations of uranium in the bismuth combined with available activity coefficient information. The activity of carbon and uranium referred to pure solid elements in the diphasic field $UC_2 + UC$ was determined as follows: T (K), x, a_C, a_U = 1165, 0.01926, 0.973, 3.269×10^{-5}; 1115, 0.01720, 0.954, 2.094×10^{-5}. The measured Gibbs energies of formation are given as follows: T (K), $\Delta G°_f(UC_2)$ (J/mol) = 1165, -100541 ± 2008; 1115, -100709 ± 1925; 1015, -100876 ± 1757. T (K), $\Delta G°_f(UC)$ (J/mol) = 1165, -100290 ± 1506; 1115, -100290 ± 1381.

MacLeod [71] calculated the molar thermodynamic properties of uranium dicarbide (300–1800 K) from enthalpy measurement (400–1520 K) in an adiabatic drop calorimeter. The heat of formation of uranium dicarbide from the solid elements was calculated at 298 K from the existing free energy data and the present enthalpy values: $\Delta H°_{298.15\ K}(UC_{1.9}) = -87864 \pm 837$ J/mol or -30298 ± 289 J/g at. Numerical results are reported in Table 14 from the original table.

The specific heat and heat content of UC were measured by Affortit [72] by using the 'rapid heating' method. Numerical results are reported in Table 15 from the original table.

Thermodynamic properties of uranium carbides UC and $UC_{1.90}$ were measured by Akhachinski and Bashlykov [73]. Thermal functions were calculated and reported in Table 16 from the original tables.

The high-temperature thermodynamic properties of hypo- and hyper-stoichiometric uranium carbides were studied by Tetenbaum and Hunt [43]. The activity of carbon was measured versus the C/U ratio in the temperature range 2155–2455 K. The calculated free energies and heats of formation are presented in Table 17. The heats of formation of $UC_{1.00}$, $UC_{1.5}$ and $UC_{1.85}$ were found by averaging values to be $\Delta H°_{f(298)}(U_{0.5}C_{0.5}) = -47488 \pm 628$ J/g at., $\Delta H°_{f(298)}(U_{0.4}C_{0.6}) = -36373 \pm$

Table 14
Thermal functions of $UC_{1.9}(U_{0.345}C_{0.655})$ versus temperature from MacLeod [71]

Experimental			Calculated			
T (K)	H_T–H_{298} (J/g at.)	S_T–S_{298} (J/g at. K)	T (K)	C_p (J/g at. K)	H_T–H_{298} (J/g at.)	$S°_T$ (J/g at. K)
402.78	2378	6.80982	298	20.92	0	23.53139
475.27	4086	10.70527	300	20.99214	39	23.61796
536.12	5646	13.79277	330	22.00207	684	25.96966
599.15	7228	16.59172	400	23.60353	2284	30.12480
679.24	9398	19.98221	500	25.04629	4722	35.92469
751.10	11260	22.60803	600	25.98408	7274	40.12312
827.81	13375	25.27713	700	26.71989	9910	44.20612
895.30	15160	27.38356	800	27.32585	12614	47.84188
980.08	17638	30.02381	900	27.87410	15374	51.10251
1040.15	19309	31.66855	1000	28.36463	18186	54.08902
1099.76	21167	33.41429	1100	28.85517	21048	56.80141
1175.80	23290	35.27545	1200	29.30243	23956	59.34066
1272.41	26191	37.64157	1300	29.74968	26909	61.69236
1412.40	30201	40.68579	1400	30.18251	29906	63.91421
1523.53	33466	42.92207	1500	30.61534	32944	65.35697
			1600	31.04817	36026	67.92508
			1700	31.45214	39149	69.78623
			1800	31.87054	42315	70.83945

Table 15
Experimental enthalpy of UC versus temperature from Affortit [72]

T (K)	C_p (J/g at. K)	H_T–H_{700} (J/g at.)
700	28.49304	0
800	29.20432	2887
900	29.93652	5837
1000	30.64778	8870
1100	31.38000	11966
1200	32.09128	15146
1300	32.82348	18395
1400	33.53476	21715
1500	34.26696	25104
1600	34.99916	28577
1700	35.75228	32112
1800	36.52632	35710
1900	37.34220	39413
2000	38.28360	43199
2100	39.37144	47070
2200	40.71032	51087
2300	42.38392	55229
2400	44.53868	59580
2500	47.36288	64162
2600	50.98204	69078
2700	55.60536	74392
2800	61.46296	80249

1450 J/g at. and $\Delta H°_{f(298)}(U_{0.351}C_{0.649}) = -33325 \pm 1908$ J/g at.

The partial Gibbs energy of carbon ΔG^C was calculated from the values of ΔH_C and ΔS_C versus temperature and composition and are reported in Table 18 from the original values.

Oetting et al. [74] determined by drop calorimetry the high-temperature enthalpy of uranium monocarbide, uranium sesquicarbide and uranium dicarbide (UC, U_2C_3, $UC_{1.90}$). Experimental results are reported in Table 19 from the original tables. The calculated heat capacity of the three uranium carbides is reported in Table 20.

The experimental enthalpy of formation and entropy at room temperature of the uranium carbides coming from various sources are reported in Table 21.

Another useful thermodynamic property, the activity of pure components (carbon and uranium), was experimentally determined and graphically reported by Storms [12] from technical reports in the temperature range 2100–2300 K and composition range $0.3 < x^{(U)} < 0.53$. The activity of uranium in the $(UC_2 - C)$ and $(UC + UC_2)$ fields and temperature range 1015–1160 K was also measured by Craig et al. [70]: T (K), $x^{(U)}$, $a_U = 1015$, 1.13×10^{-2}, 6.43×10^{-6}; 1065, 1.35×10^{-2}, 1.14×10^{-5}; 1115, 1.57×10^{-2}, 1.91×10^{-5}; 1160, 1.81×10^{-2}, 2.98×10^{-5}; 1115, 1.720×10^{-2}, 2.094×10^{-5}; 1165, 1.926×10^{-2}, 3.269×10^{-5}. The activity of carbon was measured by Tetenbaum and Hunt [43] in the temperature range 2155–2455 K and the composition range $0.35 < x^{(U)} < 0.51$ (Table 18).

Some other works have been made on calculation of thermodynamic properties from theoretical approaches.

Hoch et al. [75] used a statistical model to treat the measured carbon activity as a function of the composition and temperature in the non-stoichiometric uranium monocarbide UC_x $(x < 1)$.

Nikol'skii [76] and Nikol'skii and Levina [77] proposed equations to describe the activities of uranium

Table 16
Thermal functions of $UC(U_{0.500}C_{0.500})$ and $UC_{1.90}(U_{0.345}C_{0.655})$ versus temperature from Akhachinski and Bashlykov [73]

T (K)	$U_{0.500}C_{0.500}$			$U_{0.345}C_{0.655}$		
	C_p (J/g at. K)	H_T–H_{298} (J/g at.)	$S°_T$ (J/g at. K)	C_p (J/g at. K)	H_T–H_{298} (J/g at.)	$S°_T$ (J/g at. K)
298	25.06216	0	29.60180	20.94886	0	23.56025
500	28.43028	5477	43.55544	25.23385	4792	35.73718
700	29.68548	11301	53.34600	26.30149	9956	44.42254
900	30.62688	17332	60.91904	27.39799	15319	51.16022
1100	31.38000	23556	67.15320	29.12497	20959	56.80141
1300	32.59336	29957	72.50872	31.65412	27023	61.86549
1500	33.74396	36589	77.23664	35.05903	33680	66.62659
1700	35.08284	43472	81.54616	39.37288	41108	71.27228
1900	36.56816	50626	85.52096	44.61010	49492	75.91796
2038				48.76524	55930	79.19302
2038				42.47481	59534	80.96761
2100	38.22084	58116	89.26564	42.47481	62167	82.23724
2300	40.04088	65940	92.82204	42.47481	70661	86.04612
2500	42.04920	74141	96.25292	42.47481	79155	89.65302
2700	44.20396	82760	99.55828	42.47481		
2800				42.47481	91897	94.45741
2823	45.62652	88282	101.5666			

Table 17
Free energies and heats of formation (J/g at.) for UC_x from Tetenbaum and Hunt [43]

T (K)	2155		2255		2355		2455	
x(U)	$\Delta G°_f$	$\Delta H°_{f(298)}$	$\Delta G°_f$	$\Delta H°_{f(298)}$	$\Delta G°_f$	$\Delta H°_{f(298)}$	$\Delta G°_f$	$\Delta H°_{f(298)}$
0.50505	–	–	−48870	−45644	−49447	−45432	−51560	−47968
0.50000	−52509	−48116	−51882	−47488	−51672	−47488	−51254	−46861
0.48780	−43677	−38779	−45922	−41024	−47146	−42248	−48167	−43473
0.47619	−48663	−41840	−49013	−43633	−50606	−43832	−51403	−45626
0.46512	–	–	−49040	−43202	−50208	−44175	−52154	−46121
0.45455	–	–	–	–	−49067	−42601	−50779	−44122
0.43478	–	–	–	–	–	–	−49662	−42022
0.41667	–	–	–	–	−45850	−37482	−48465	−40445
0.40000	–	–	−44016	−35313	−45187	−35982	−47363	−37824
0.38462	–	–	−43127	−33794	−44898	−34920	−46668	−36208
0.37736	−39314	−37103	–	–	–	–	–	–
0.37037	−46334	−37036	−41840	−31767	−44009	−33317	−44939	−33627
0.35714	−45725	−36012	−41691	−31081	−42438	−31081	−43036	−30932
0.35088	−45217	−35234	–	–	−42562	−31416	–	–

Table 18
Partial Gibbs energy of carbon ΔG_C (J/mol) from Tetenbaum and Hunt [43]

x(U)	ΔG_C			
	2155 K	2255 K	2355 K	2455 K
0.51020	−28397	−23497	−18602	−13707
0.50505	−12008	−9498	−6987	−4477
0.48780	−4335	−11991	−19648	−27309
0.48077	−4100	−10795	−17489	−24183
0.47619	−3803	−10037	−16271	−22506
0.47393	−3481	−9506	−15531	−21556
0.36900	−3579	−6966	−10355	−13744
0.35971	−3349	−6318	−9288	−12259
0.35088	−2406	−4498	−6590	−8682

and carbon as a function of the composition of a cubic solid solution of UC_y. Formally, it corresponded to an ideal solution of U, UC and UC_2 with a reaction $UC_2 + U \Longleftrightarrow 2UC$.

Murch and Thorn [78] described the partial molar properties of carbon in UC_x $(1 < x < 2)$ in terms of an fcc lattice gas model in which the C_2 groups attract only when they are nearest neighbours. The chemical potential was calculated by using a modified Monte-Carlo method.

McLellan [79,80] applied to the $UC_{1\to2}$ phase the method of expanding the free energy of a solid solution crystal in terms of semi-invariant cumulants as the high-temperature limit is approached. The rock-salt-like

Table 19
Enthalpy of $UC(U_{0.500}C_{0.500})$, $U_2C_3(U_{0.400}C_{0.600})$ and $UC_{1.90}(U_{0.345}C_{0.655})$ versus temperature from Oetting et al. [74]

$U_{0.500}C_{0.500}$		$U_{0.400}C_{0.600}$		$U_{0.345}C_{0.655}$	
T (K)	H_T–H_{298} (J/g at.)	T (K)	H_T–H_{298} (J/g at.)	T (K)	H_T–H_{298} (J/g at.)
501.3	5560	429.8	3020	467.0	3835
522.3	6123	503.5	4792	570.8	6382
625.4	9217	570.8	6471	573.1	6528
644.4	9682	633.6	8144	623.8	7842
719.6	12075	693.6	9746	650.3	8420
738.5	12671	698.6	9913	670.0	8963
738.6	12750	775.9	11956	670.7	9036
798.4	14474	831.3	13477	672.9	9113
870.6	16799	900.5	15395	725.2	10572
871.1	16591	924.1	16053	774.6	11779
943.4	18986	971.9	17374	775.7	11783
1021.3	21426	1009.5	18425	829.5	13282
1091.3	23568	1044.1	19505	875.6	14543
1169.5	26110	1131.2	21771	883.8	14785
1252.0	28842	1141.6	22085	936.0	16338
1352.7	32313	1213.0	24428	989.6	17770
1448.6	35719	1280.9	26455	1001.8	17970
1455.4	35842	1298.4	26837	1045.3	19449
1571.0	39982	1346.4	28275	1075.3	20145
1672.0	43392	1351.1	28386	1090.2	20542
		1351.2	28417	1096.5	20821
		1367.4	29121	1147.1	22480
		1435.7	31721	1147.6	22277
		1499.9	33831	1168.8	22937
		1567.4	35818	1201.1	24053
		1667.4	39394	1278.8	26463
				1312.3	27427
				1362.0	29006
				1543.2	34231
				1670.3	37699

structure contained linked C–C pairs in octahedral sites in the fcc Bravais lattice.

2.3. Thermodynamic modelling and optimization results

The liquid phase, L, was described by a substitutional model with one lattice, with the following formula $[C_1, U_1]_1\langle L\rangle$. A Redlich–Kister polynomial of third order was used for the excess Gibbs energy interaction parameter, $L_{-}[C_1, U_1]_1\langle L\rangle$.

The $C_{1\pm x}U_1(UC, UC_2)$ solid solution, fcc_B1 or δ, was described by a two-sublattice model. The following formula was used: $[C_1, C_2, Va]_1[U_1]_1\langle fcc\_B1\rangle$. The first lattice may be occupied by single carbon atoms, C_1, double carbon atoms, C_2 or vacancies, Va. Such a description allowed us to describe both the $C_{1-x}U_1$ composition range, i.e. the domain UC–U, and the $C_{1+x}U_1$ composition range, i.e. the domain UC–UC_2. The first domain is covered by the part of the formula $[C_1, Va]_1[U_1]_1\langle fcc\_B1\rangle$, in which reference components are $C_1U_1(fcc\_B1, \delta)$ and $U_1(fcc\_B1, \delta)$, while the second domain is covered by the part of the formula $[C_1, C_2]_1[U_1]_1\langle fcc\_B1\rangle$, in which reference components are $C_1U_1(fcc\_B1, \delta)$ and $C_2U_1(fcc\_B1, \delta$ or $\beta)$. Thus, the first excess Gibbs energy interaction parameter $L[C_1, Va]_1[U_1]_1\langle fcc\_B1\rangle$ allowed us to describe the sub-stoichiometry of UC with respect to carbon, and the second one, $L[C_1, C_2]_1[U_1]_1\langle fcc\_B1\rangle$ the over-stoichiometry of UC up to UC_2. This interaction term also allowed us to represent the solid miscibility gap between (UC) and (UC_2) below 2373 K. The first interaction term was described by a constant term versus composition (regular description), and the second one by a first-order Redlich–Kister polynomial (sub-regular description). The interaction term $L[C_2, Va]_1[U_1]_1\langle fcc\_B1\rangle$ was set to zero, because the occupancy of Va is very small when C_1, C_2 are simultaneously present, as the one of C_2 when C_1 and Va are simultaneously present. The Gibbs energy of the fictive $U_1(fcc\_B1, \delta)$ structure was set to a positive value (20 000 J) to be metastable at any temperature. The other reference component $C_1U_1(fcc\_B1, \delta)$ is a stable one, while $C_2U_1(fcc\_B1, \delta$ or $\beta)$ is metastable but near the stable compound $UC_{1.90–1.93}$ (high-temperature form).

Table 20
Heat capacity of $UC(U_{0.500}C_{0.500})$, $U_2C_3(U_{0.400}C_{0.600})$ and $UC_{1.90}(U_{0.345}C_{0.655})$ versus temperature calculated by Oetting et al. [74] from the experimental enthalpy

T (K)	$C_p(U_{0.5}C_{0.5})$ (J/g at. K)	$C_p(U_{0.4}C_{0.6})$ (J/g at. K)	$C_p(U_{0.345}C_{0.655})$ (J/g at. K)
298	25.06216	21.47288	20.87686598
300	25.104	21.489024	20.90562199
400	27.59348	23.991056	23.11983505
500	28.78592	25.087261	24.55763574
600	29.51812	25.748336	25.67912027
700	30.06204	26.292256	26.61369072
800	30.50136	26.852912	27.4188591
900	30.91976	27.497248	28.12338144
1000	31.31724	28.242	28.74163574
1100	31.75656	29.12064	29.288
1200	32.19588	30.149904	29.76247423
1300	32.65612	31.313056	30.16505842
1400	33.1582	32.6352	30.51013058
1500	33.70212	34.116336	30.78331271
1600	34.28788	35.756464	30.98460481
1700	34.89456	37.555584	
1800	35.54308	39.513696	
1900	36.23344	41.5028	
2000	36.98656	43.923632	
2100	37.7606		
2200	38.57648		
2300	39.4342		
2400	40.33376		
2500	41.27516		
2600	42.2584		
2700	43.28348		
2800	44.3504		
2823	44.62236		

The low-temperature form of the $C_{1+x}U_1(UC, UC_2)$ solid solution, bct or α, was described similarly to the high-temperature form, by a two-sublattice model, with the same formula, $[C_1, C_2, Va]_1[U_1]_1\langle bct\rangle$. The interaction parameters were taken identical to the ones of the fcc_B1 phase, as the Gibbs energy of the hypothetical reference states $U_1(bct, \alpha)$ and $U_1(fcc\_B1, \delta)$. Thus, the difference of Gibbs energy of the fcc_B1 and bct solid solutions came only from the one of the reference substances, $C_2U_1(fcc\_B1, \delta \text{ or } \beta)$ and $C_1U_1(fcc\_B1, \delta)$ on the one hand, $C_2U_1(bct, \alpha)$ and $C_1U_1(bct, \alpha)$ on the other hand. Because the low-temperature form appears only near the (UC_2)-rich compositions, the Gibbs energy of $C_1U_1(bct, \alpha)$ was chosen in order that this compound be metastable.

The difference of the Gibbs energies of $C_2U_1(fcc\_B1, \delta \text{ or } \beta)$ and C_2U_1 (bct or α) allowed us to reproduce the selected transition temperatures observed on the phase diagram between the low-temperature and the high-temperature form.

The sesquicarbide phases ε-C_3U_2 were considered as a stoichiometric compound.

ε-C_3U_2 and the pure stable reference substances $C_1U_1(fcc\_B1, \delta)$, $C_2U_1(fcc\_B1, \delta \text{ or } \beta)$ and C_2U_1 (bct or α) were described by a six-term function versus temperature. Their Gibbs energies were optimized from the experimental thermodynamic data of pure substances.

In the optimization process, a primary criticism of the available experimental information was firstly made and experimental values which were evidently out of range of the currently accepted ones were discarded before running the assessment code. All other experimental values (phase diagram and thermodynamic properties) were taken into account in the optimization process.

All Gibbs energy parameters Appendices A–D will be stored in the THERMALLOY solution thermodynamic database [97].

The SGTE 'lattice-stabilities' of pure elements are reported in Appendix A. The estimated 'lattice-stabilities' and the optimized Gibbs energy parameters of stoichiometric compounds are reported in Appendix B. The excess Gibbs energy interaction parameters of solution phases are reported in Appendix C. The fundamental thermodynamic properties of stoichiometric compounds are reported in Appendix D.

The entire C–U phase diagram was calculated with the optimized Gibbs energy parameters obtained in this work and compared to the selected experimental information in Fig. 3. The overall agreement is quite

Table 21
Comparison of calculated enthalpy of formation and entropy at room temperature, $\Delta H°_{f(298)}$ in J/g at. and $S°_{(298)}$ in J/g at. K, for the stoichiometric compounds, $UC(C_{0.500}U_{0.500})$, $UC_{1.90}(C_{0.655}U_{0.345})$ and $U_2C_3(C_{0.600}U_{0.400})$, and experimental ones

$C_{0.500}U_{0.500}$			$C_{0.655}U_{0.345}$			$C_{0.600}U_{0.400}$		
x	$\Delta H°_{f(298)}$	Reference	x	$\Delta H°_{f(298)}$	Reference	x	$\Delta H°_{f(298)}$	Reference
0.50	-43932 ± 2092	[52]	0.34	−31798	[58]	0.40	-36373 ± 1450	[43]
0.50	−41422	[53]	0.34	−30962	[60]			
0.50	−34727[a]	[54]	0.35	−31380	[62]			
0.52	−46861	[55]	0.36	−31798	[63]			
0.50	−35146[a]	[56]	0.34	−18410[a]	[54]			
0.50	−48534	[57]	0.34	−27614[a]	[61]			
0.50	−48534	[12]	0.34	−33890	[65]			
0.50	-47488 ± 628	[43]	0.34	−31380	[57]			
			0.34	−30125	[66]			
			0.345	-28422 ± 4404[a]	[64]			
			0.345	-26835 ± 2885[a]	[64]			
			0.345	-30442 ± 2020	[64]			
			0.351	-33325 ± 1908	[43]			
			0.345	-30298 ± 289	[71]			
0.50	-48534 ± 2092	[11]	0.34	-30543 ± 2929	[11]	0.40	-41003 ± 3347	[11]
0.50	−48534	[calc.]	0.345	−30533	[calc.]	0.40	−38349	[calc.]
x	$S°_{(298)}$	Reference	x	$S°_{(298)}$	Reference	x	$S°_{(298)}$	Reference
0.50	29.87376	[69]	0.341	24.07585	[69]	0.40	27.57256	[11]
0.50	29.60180	[74]	0.345	23.53139	[71]	0.40	27.55582	[74]
0.50	29.60180	[73]	0.345	23.47928	[74]			
0.50	29.87376	[11]	0.345	23.56025	[73]			
			0.34	23.22120	[11]			
0.50	29.87376	[calc.]	0.345	23.973	[calc.]	0.40	26.68	[calc.]

[a] Discarded.

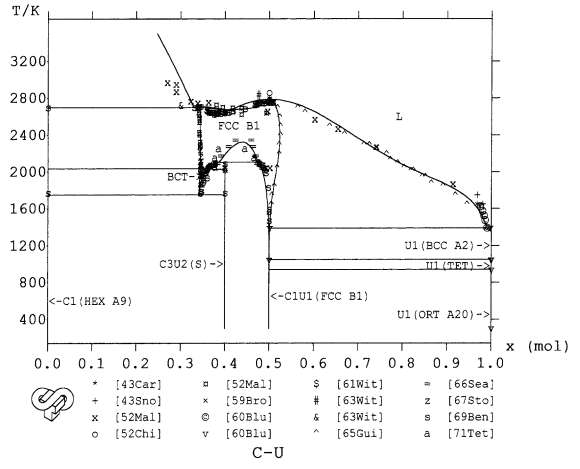

Fig. 3. Calculated C–U equilibrium phase diagram (this work) compared to experimental information.

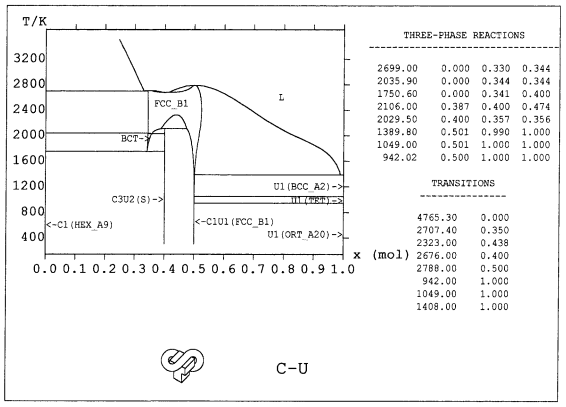

Fig. 4. Calculated C–U equilibrium phase diagram (this work) with quoted invariant or transition reactions.

satisfactory, whatever the agreement is better with the phase diagram presented by Benz et al. [14] in Fig. 2 than with the one presented by Storms [12] in Fig. 1. The calculated phase diagram is presented with the quoted compositions and temperatures of all assessed invariant reactions or transitions in Fig. 4 and with different axes (C/U mol ratio, temperature in °C) in Fig. 5. The calculated reactions were compared to the experimental ones in Table 2.

The enthalpy of formation $\Delta H°_{f(298)}$ and entropy at room temperature, $S°_{(298)}$ of the uranium carbides UC, U_2C_3 and $UC_{1.90}$ were calculated and compared to the

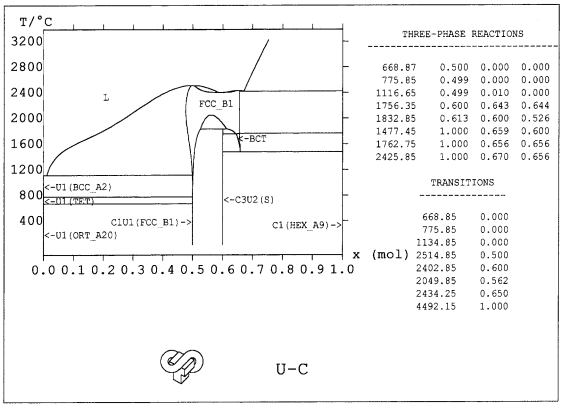

Fig. 5. Calculated C–U equilibrium phase diagram (this work) with different axes.

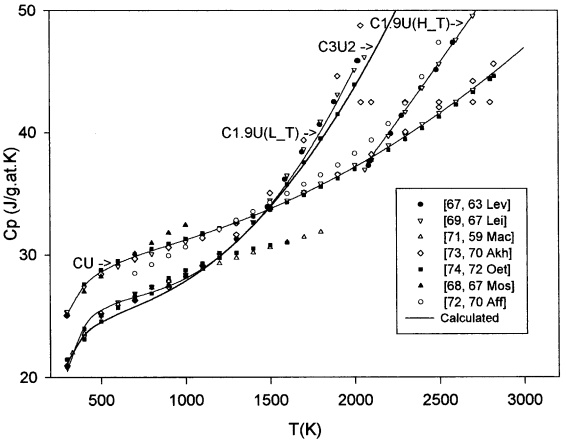

Fig. 6. Calculated heat capacity of the three uranium carbides, UC, U_2C_3 and $UC_{1.9}$, compared to the experimental information from various sources.

experimental ones in Table 21. The calculated heat capacity compared to the various experimental data is presented in Fig. 6.

The heat content versus temperature H_T–H_{298} of the three uranium carbides was compared to the available experimental data in Tables 22–24 and Figs. 7–9.

The activity of C and U was calculated at 2100 and 2300 K and compared to the experimental data taken from Storms [12] in Figs. 10 and 11.

3. The B–U system

3.1. Short presentation of the different phases

The phase diagram of the B–U binary system was reported in a compilation work by Elliott [9]. Hansen and Anderko [8] and Shunk [10] only gave information on the intermediate phases and the invariant reactions or melting points. The B–U phase diagram taken from Elliott [9] is presented in Fig. 12.

The condensed solutions and stoichiometric substances, with the symbols currently used in this work, are as follows: liquid phase, L; intermediate compounds $B_{12}U_1(S)$ or UB_{12}, $B_4U_1(S)$ or UB_4, $B_2U_1(S)$ or UB_2; pure uranium: U_1(ort_A20) or α-U; U_1(tet) or β-U; U_1(bcc_*A2*) or γ-U; pure boron: B_1(rho) or B. No mutual solubility of boron in uranium and uranium in boron was reported.

The three compounds melt congruently and the diagram shows four eutectic reactions.

The structures of the intermetallic compounds were given by Hansen and Anderko [8] and Elliott [9] and reported in Table 25.

3.2. Experimental information

In the following, T is the temperature in Kelvin (Celsius are quoted between brackets), x(U) or x the uranium atomic fraction in one phase, x^G is the global uranium atomic fraction, L the liquidus or the liquid, and S the solidus. In all tables, values between brackets are not experimental but estimated for the optimization.

3.2.1. Phase diagram

According to Hansen and Anderko [8], the temperature of the U–UB_2 eutectic is close to 1405 K (1132°C), while the one of the UB_2–UB_4 eutectic is above 1838 K (1565°C).

The diagram reported by Elliott [9] is mainly based on the experimental study of Howlett [84] by means of X-ray, metallographic and dilatometric techniques. The melting points of uranium–boron alloys were determined by optical measurements and reported in Table 26. The solid solubility of boron in uranium is low. The U–UB_2 eutectic temperature was located at 1380.65 ± 2.5 K (1107.5°C) by metallographic indications of melting after annealing, the composition near 2 at.% boron by metallographic evidence of proeutectic constituents. The melting point of UB_2 was located near 2703 K (2430°C). UB_4 melted at 2768 K (2495°C), and UB_{12} at 2508 K (2235°C). A narrow homogeneity range was observed for UB_2, due to the presence of vacancies on the uranium sublattice. The temperature of the β-U $\Longleftrightarrow$ α-U + UB_2 eutectoid reaction is located at 928 K (655°C), the one of the γ-U $\Longleftrightarrow$ β-U + UB_2 transformation at 1043 K (770°C).

According to Eding and Carr [85], UB_{12} apparently decomposed at 1673 K (1400°C).

Shunk [10] reported the melting temperatures for UB_2 (2433 K or 2160°C) and UB_4 (2403 K or 2130°C) considerably lower than those given by Howlett [84].

The B-rich portion of the system was investigated by Mar [86] who determined the eutectic (mean value 2309

Table 22
Comparison of calculated heat content versus temperature of the uranium monocarbide UC and experimental ones, $H_T-H_{298}(C_{0.500}U_{0.500})$ in J/g at.

T (K)	$H_T-H_{298}(C_{0.500}U_{0.500})$ (J/g at.)				
	[68]	[69]	[73]	[74]	Calculated
298	0	0	0	0	0
300		46		50	46
400	2678	2699		2699	2679
500	5439	5489	5477	5525	5472
600	8326	8364		8443	8356
700	11297	11299	11301	11424	11303
800	14351	14282		14451	14302
900	17489	17315	17332	17523	17349
1000	20711	20395		20635	20441
1100		23522	23556	23788	23580
1200		26704		26985	26768
1300		29939	29957	30227	30006
1400		33229		33518	33297
1500		36581	36589	36863	36645
1600		39995		40260	40053
1700		43474	43472	43720	43524
1800		47024		47242	47061
1900		50645	50626	50831	50670
2000		54342		54492	54352
2100		58114	58116	58229	58112
2200		61970		62044	61953
2300		65908	65940	65944	65880
2400		69932		69931	69896
2500		74046	74141	74011	74004
2600		78251		78186	78210
2700		82550	82760	82462	82515
2800		86948		86843	86926
2823			88282	87889	87955

K or 2036°C) and liquidus temperatures (reported in Table 26) from cooling curves. The phase relations were determined primarily by a thermal analysis technique in which an optical pyrometer was used as the sensor.

3.2.2. Thermodynamic properties

Podobeda and Malykh [87] determined theoretically the standard values of the entropy and the temperature dependence of the heat capacity of uranium borides. They used both new approaches as well as most of the currently known methods of calculating by empirical formula. The entropy at room temperature, $S°_{298.15\ K}$ was reported as follows: UB_2: 12.4, 16.62, 15.6, 15.28, 15.15, 14.81, 15.21 cal/mol K, mean value: 15.01 cal/mol K, 20.934 J/g at. K; UB_4: 22.25, 22.3, 16.52, 16.53, 19.60, 18.74 cal/mol K, mean value: 19.32 cal/mol K, 16.17 J/g at. K; UB_{12}: 37.2, 30.47, 20.57, 36.74, 27.17 cal/mol K, mean value: 30.43 cal/mol K, 9.794 J/g at. K. They gave up to four equations for the temperature dependence of each uranium boride, corresponding to the different models.

Flotow et al. [88] prepared a sample of uranium diboride characterized as $UB_{1.979\pm0.006}$. They measured the standard enthalpy and entropy of UB_2 at room temperature, $\Delta H°_{f,298.15\ K} = -54810 \pm 5579$ J/g at., $\Delta S°_{f,298.15\ K} = -2.148 \pm 0.07$ J/g at. K. They reported the values from Alcock and Grieveson [89] calculated from equilibrium measurements at high temperature: $\Delta H°_{f,298.15\ K} = -48255 \pm 4184$ J/g at., $\Delta S°_{f,298.15\ K} = +0.7 \pm 2.8$ J/g at. K. At 298.15 K, the heat capacity, the entropy and enthalpy increment were determined as $C_{p,298.15\ K} = 18.587 \pm 0.037$J/g at. K, $S°_{298.15\ K} = 18.503 \pm 0.037$ J/g at. K, $H_T - H_0 = 2960 \pm 6$ J/g at. The heat capacity was measured from 7.43 to 348.31 K. Experimental results above 298.15 K are reported in Table 27.

Fredrickson et al. [90,91] measured the enthalpy of uranium diboride from 600 to 1500 K and from 1300 to 2300 K, respectively, by drop calorimetry and tabulated the thermodynamic functions of $UB_{1.98}$ from the experimental values. Experimental and calculated values are reported in Table 28 and 29, respectively.

Mar and Stout [92] determined the enthalpy of the uranium dodecaboride from 1300 to 2200 K by drop calorimetry. Experimental results are given in Table 30.

Table 23
Comparison of calculated heat content versus temperature of the uranium dicarbide $UC_{1.90–1.93}$ and experimental ones, $H_T–H_{298}(UC_{1.90–1.93})$ in J/g at. (low-temperature form up to 2038 or 2060 K)

x(U)	0.341	0.345	0.345	0.344	0.345
T (K)	$H_T–H_{298}(UC_{1.90–1.93})$ (J/g at.)				
	[69]	[71]	[73]	[74]	Calculated
298	0	0	0	0	0
300	39	39		42	38
400	2258	2284		2250	2295
500	4682	4722	4792	4637	4775
600	7244	7274		7152	7353
700	9895	9910	9956	9767	9989
800	12606	12614		12470	12669
900	15367	15374	15319	15248	15395
1000	18177	18186		18092	18177
1100	21047	21048	20959	20995	21027
1200	23999	23956		23948	23960
1300	27056	26909	27023	26944	26992
1400	30250	29906		29978	30143
1500	33608	32944	33680	33044	33432
1600	37153	36026		36132	36877
1700	40910	39149	41108		40499
1800	44889	42315			44319
1900	49091		49492		48356
2000	53507				52630
2038			55930		54321
2060	56247				55318
2038			59534		59492
2060	60175				60211
2100	61670		62167		61702
2200	65545				65552
2300	69616		70661		69579
2400	73883				73785
2500	78348		79155		78173
2600	83009				82745
2700	87868				87503
2800	92923		91897		92448
2900	98175				97583
3000	103625				102908

Borovikova and Fesenko [93] evaluated the standard entropy for uranium borides by a method of comparative calculations as $S°_{298.15\ K} = UB_{12} : 8.688 \pm 0.961$ J/g at. K; $UB_4 : 15.058 \pm 1.674$; $UB_2 : 18.377 \pm 0.043$ J/g at. K.

Chipaux et al. [94] measured the heat capacity of UB_4 up to 1100 K and analyzed the variation versus temperature following a law of type $C_p = 24.189 + 0.03791T - 708810/T^2$ J/g at. K. They also reported three experimental values from Krikorian [95].

The heat capacity values of B_4U given by Chipaux et al. [94] differ strongly from the ones reported by Krikorian [95] and those estimated by using the Neumann–Kopp rule between U(ort_A20) and B(beta_rho_B), graphically represented in Fig. 17.

Moreover, the estimated heat capacity of $B_{12}U$ is in agreement with the experimental heat content $H_T–H_{298.15}$ determined by Mar and Stout [92], as presented in Fig. 18.

The enthalpies and entropies of formation of B_2U, B_4U and $B_{12}U$ were reported by Potter [96] as −54810, 18.367; −49120, 14.226; −33311, 10.75 J/g at. and J/g at. K, respectively.

3.3. Thermodynamic modelling and optimization results

The liquid phase, L, was described by a substitutional model with one lattice, with the following formula $[B_1, U_1]_1\langle L\rangle$. A Redlich–Kister polynomial of second-order (sub-regular) was used for the excess Gibbs energy interaction parameter, $L\_[B_1, U_1]_1\langle L\rangle$.

The three uranium borides, UB_{12}, UB_4 and UB_2 were all considered as stoichiometric compounds, although a

Table 24
Comparison of calculated heat content versus temperature of the uranium sesquicarbide U_3C_3, and experimental ones, $H_T–H_{298}(C_{0.4}U_{0.6})$ in J/g at.

T (K)	$H_T–H_{298}(C_{0.4}U_{0.6})$ (J/g at.)	
	[74]	Calculated
298	0	0
300	26	40
400	2335	2333
429.8	3020	3053
500	4795	4790
503.5	4792	4878
570.8	6471	6584
600	7337	7332
633.6	8144	8200
693.6	9746	9766
698.6	9913	9897
700	9940	9934
775.9	11956	11946
800	12587	12591
831.3	13477	13435
900	15313	15308
900.5	15395	15322
924.1	16053	15973
971.9	17374	17305
1000	18099	18096
1009.5	18425	18364
1044.1	19505	19350
1100	20967	20964
1131.2	21771	21878
1141.6	22085	22185
1200	23982	23928
1213	24428	24321
1280.9	26455	26406
1398.4	26837	26952
1300	27001	27002
1346.4	28275	28469
1351.1	28386	28619
1351.2	28417	28623
1367.4	29121	29143
1400	30197	30200
1435.7	31721	31374
1499.9	33831	33534
1500	33534	33537
1567.4	35818	35874
1600	37026	37030
1667.4	39394	39480
1700	40690	40694
1800	44543	44545
1900	48599	48599
2000	52876	52872

very narrow stoichiometry range was probable for UB_2, but without accurate limits.

In the optimization process, the Gibbs energy of UB_2 was first evaluated by taking into account the standard enthalpy and entropy at room temperature of Flotow et al. [88] and the enthalpy and heat capacity (600–2300 K) of Fredrickson et al. [90,91]; it was fixed as

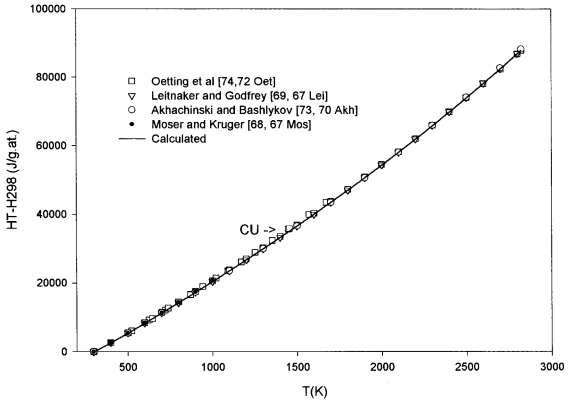

Fig. 7. Calculated heat content of the uranium carbide, UC, compared to the experimental information from various sources.

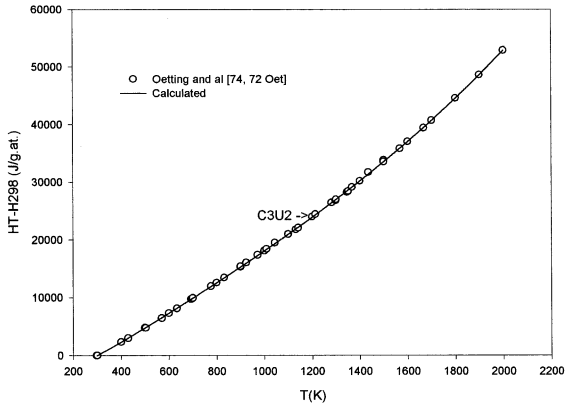

Fig. 8. Calculated heat content of the uranium carbide, U_2C_3, compared to the experimental information from various sources.

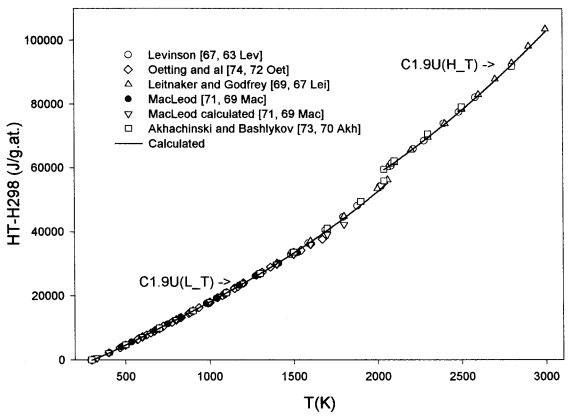

Fig. 9. Calculated heat content of the uranium carbide, $UC_{1.9}$, compared to the experimental information from various sources.

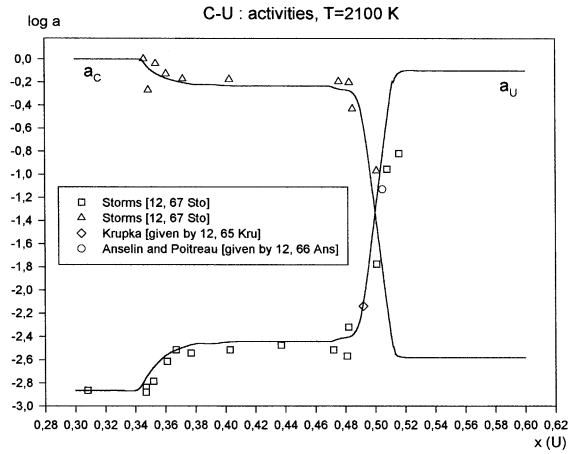

Fig. 10. Calculated activity of uranium and carbon at 2100 K compared to the experimental data reported by Storms [12].

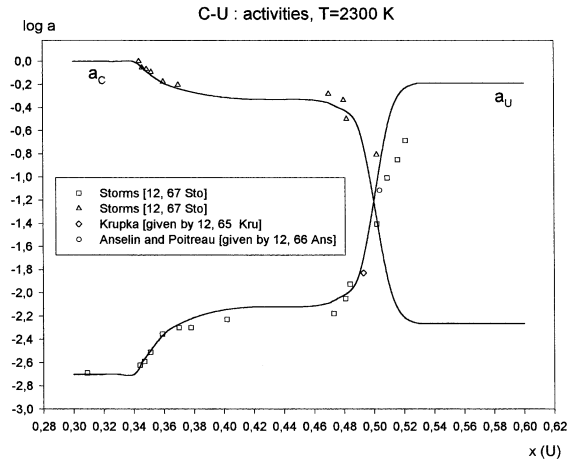

Fig. 11. Calculated activity of uranium and carbon at 2300 K compared to the experimental data reported by Storms [12].

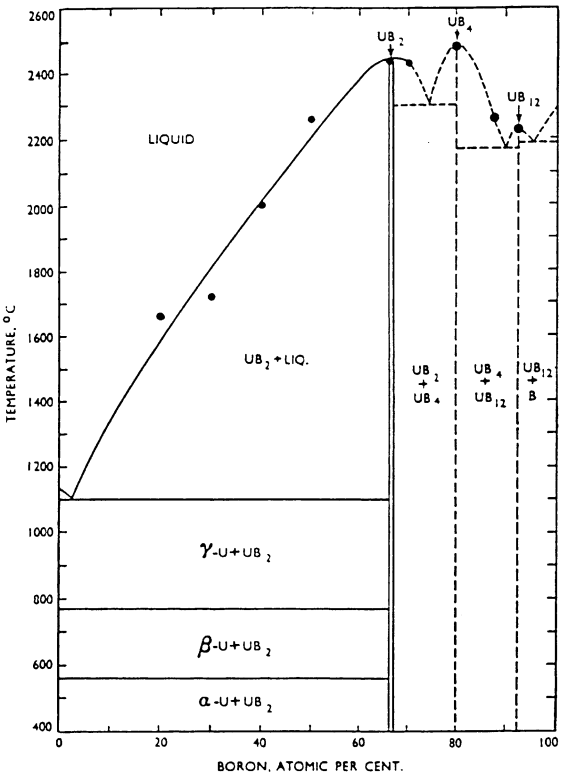

Fig. 12. Phase diagram of the U–B system taken from Howlett et al. [84].

follows. The heat capacity data of Chipaux et al. [94] for UB_4 were found to be inconsistent with the other values and thus discarded. The heat capacities of UB_4 and UB_{12} were estimated by the Neuman–Kopp rule from U_1(ort_A20) and B_1(beta_rho_B) which agreed well with the experimental enthalpy at high temperature (1300–2200 K) for UB_{12}. The standard enthalpy of formation and entropy at room temperature of these two

Table 25
Crystal characteristics of the stoichiometric compounds in the B–U system

Compound	Structure	Lattice parameter	Reference
UB_{12}	fcc, isotypic with ZrB_{12}, 4 molecules per unit cell	$a = 7.473$ Å	[82]
		$a = 7.468$ Å	[83]
		$a = 7.4773 \pm 0.0005$ Å	[84]
UB_4	Tetragonal, isotypic with ThB_4	$a = 7.075$ Å, $c = 3.979$ Å, $c/a = 0.562$	[81]
		$a = 7.066$ Å, $c = 3.97$ Å, $c/a = 0.56$	[82]
		$a = 7.080$ Å, $c = 3.978$ Å, $c/a = 0.562$	[83]
UB_2	Hexagonal, isotypic with $AlB_2(C_{32})$	$a = 3.136$ Å, $c = 3.988$ Å, $c/a = 1.272$	[81]
		$a = 3.1293 \pm 0.0003$ Å, $c = 3.9893 \pm 0.0005$ Å, $c/a = 1.275$ (B-rich)	[84]
		$a = 3.1314 \pm 0.0003$ Å, $c = 3.9857 \pm 0.0005$ Å, $c/a = 1.273$ (U-rich)	

Table 26
Melting points of uranium-boron alloys from Howlett [84] and Mar [86]

T^L (K)	t^L (°C)	$x^{\phi 1}$(U)	$x^{\phi 2}$(U)	Equilibrium
[84]				
1380	1107	0.980	(0.333)	$L(\phi 1) + UB_2(\phi 2) + \gamma$-$U(\phi 3)$
1933	1660	0.812	(0.333)	$L(\phi 1) + UB_2(\phi 2)$
2048	1775	0.746	(0.333)	–
2273	2000	0.648	(0.333)	–
2533	2260	0.527	(0.333)	–
2658	2385	0.415	(0.333)	–
2703	2430	0.326	(0.333)	–
2613	2340	0.267	(0.333)	–
2663	2370	0.245	(0.200)	$L(\phi 1) + UB_4(\phi 2)$
2768	2495	0.185	(0.200)	–
2548	2275	0.126	(0.200)	–
2508	2235	0.080	(0.077)	$L(\phi 1) + UB_{12}(\phi 2)$
[86]				
2406	2133	0.055	(0.077)	$L(\phi 1) + UB_{12}(\phi 2)$
2409	2136	0.047	(0.077)	
2367	2094	0.038	(0.077)	
2348	2075	0.020	(0.077)	
2298	2025	0.009	(0.077)	
2309	2036	0.009	(0.077)	$L(\phi 1) + UB_{12}(\phi 2) + B(\phi 3)$

Table 27
Experimental heat capacity of B_2U versus temperature from Flotow et al. [88]

T (K)	C_p (J/g at. K)
298.15	18.587
300.4	18.684
310.6	19.087
320.84	19.510
330.94	19.889
340.91	20.245
348.31	20.490

compounds were then estimated in consistency with the remaining experimental information. The Gibbs energy of the uranium borides is described by a six-term function versus temperature and referred to the SER reference state. Two temperature ranges were needed to describe the heat capacity of UB_2.

All Gibbs energy parameters (Appendices A–D) will be stored in the THERMALLOY solution database [97].

The SGTE 'lattice-stabilities' of pure elements are reported in Appendix A. The estimated 'lattice-stabilities' and the optimized Gibbs energy parameters of stoichiometric compounds are reported in Appendix B. The excess Gibbs energy interaction parameters of solution phases are reported in Appendix C. The fundamental thermodynamic properties of stoichiometric compounds are reported in Appendix D.

The entire B–U phase diagram was calculated with the optimized Gibbs energy parameters obtained in this work and compared to the selected experimental information in Fig. 13. The overall agreement is quite satisfactory. The calculated phase diagram is presented with the quoted compositions and temperatures of all assessed invariant reactions or transitions in Fig. 14 and with different axes (temperature in °C, x(B)) in Fig. 15.

The calculated heat capacity C_p of UB_2 is compared to the experimental values of Flotow et al. [88] and Fredrickson et al. [90,91] in Fig. 16.

The heat content versus temperature, H_T–H_{298}, of the uranium borides UB_2 and UB_{12} was calculated and compared to the experimental ones in Tables 28 and 30.

The estimated heat capacity and the calculated heat content of the uranium borides are compared to the experimental information in Figs. 17 and 18.

4. Conclusion

We have presented in this work the critical assessment of the two binary systems B–U and C–U from all the available experimental information concerning both phase diagram and thermodynamic properties. The thermodynamic modelling of binary or ternary chemical systems including uranium and other elements (Fe, Cr, Ni, Zr, ...,) is being performed in the framework of the development of a NTD, for increasing the basic knowledge of key phenomena which may occur in the event of a severe accident in a nuclear power plant. B and C are present in the B_4C control rods of a nuclear reactor. The self-consistency obtained between the experimental results and the calculated ones by using the

Table 28
Experimental enthalpy of B_2U from Fredrickson et al. from 600 to 1500 K [90] and from 1300 to 2300 K [91]

T (K)	H_T–H_{298} (J/g at.)	
	[90]	Calculated
579.3	6342	6396
669.5	8730	8760
723.9	10209	10231
772.7	11618	11577
826.2	13069	13077
871.2	14329	14359
940.1	16328	16352
1021.7	18755	18758
1087.6	20787	20733
1135.8	22195	22195
1187.2	23759	23769
1189.8	23819	23849
1240.7	25452	25422
1293.5	27095	27068
1338.1	28495	28469
1386.9	29977	30012
1435.9	31576	31571
1485.8	33165	33169
T (K)	[91]	Calculated
1303	27327	27366
1397	30066	30332
1496	33487	33497
1604	37035	36989
1679	39189	39466
1814	43585	44122
1896	47059	47099
1991	50699	50726
2110	55265	55611
2206	59767	59897
2300	64623	64459

Table 29
Calculated heat capacity of B_2U by Fredrickson et al. from experimental enthalpy (600–1500 K [90], 1300–2300 K [91])

T (K)	C_p (J/g at. K) [90]
298.15	18.575
300	18.660
400	22.085
500	24.234
600	25.806
700	27.056
800	28.095
900	28.965
1000	29.709
1100	30.341
1200	30.861
1300	31.296
1400	31.633
1500	31.899
T (K)	C_p (J/g at. K) [91]
1500	31.942
1600	32.742
1700	33.823
1800	35.283
1900	37.179
2000	39.594
2100	42.598
2200	46.263
2300	50.657
2400	55.880
2500	61.973

Table 30
Experimental enthalpy of $B_{12}U$ from Mar and Stout [92] compared to the calculated one (this work)

T (K)	H_T–H_{298} (J/g at.)	
	[92] exp.	Calculated
1324	23577	23328
1426	26230	26186
1526	28740	29045
1626	31660	31957
1726	34680	34918
1834	37810	38166
1950	41440	41707
2046	44840	44676
2138	47490	47550
2224	50130	50259

assessed Gibbs energy parameters of the different phases is satisfactory. The fundamental thermodynamic functions (heat capacity, enthalpy of formation and entropy at room temperature) of the stoichiometric compounds $C_2U_1(S)$, $C_1U_1(S)$, $C_3U_2(S)$, $B_2U_1(S)$, $B_{12}U_1(S)$ and $B_4U_1(S)$ were assessed. However, some lack of experimental information were put in evidence, as thethermodynamic properties of the two last compounds or the liquid phases. New experimental data could be obtained in the framework of the future nuclear safety programmes and used to improve the reliability of the Gibbs energy functions.

Acknowledgements

This work was executed under the multipartner project 'ENTHALPY', co-financed by the European Commission, (European Nuclear Thermodynamic Database validated and applicable in severe accident codes) under the fifth Framework Programme of the Euratom for Research and Training in the Field of Nuclear Energies (1998–2002). The authors wish to thank the partners of this contract (IPSN, CEA, AEA-T, THERMODATA, Siemens KWU, CEA/DRN/DTP, EDF/D-R&D, Aeki, Skoda-UJP, SCK-CEN, ULB, UCL) for the valuable technical discussions.

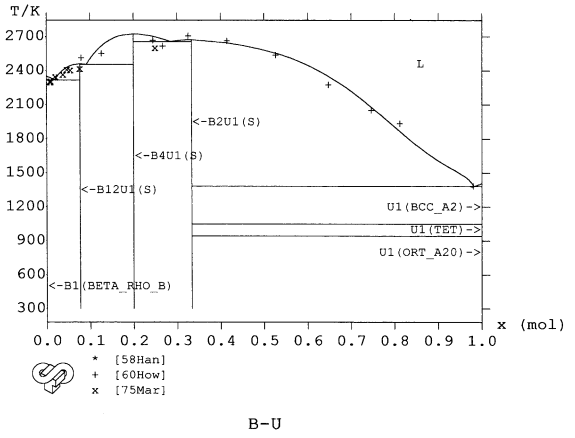

Fig. 13. Calculated B–U equilibrium phase diagram (this work) compared to experimental information.

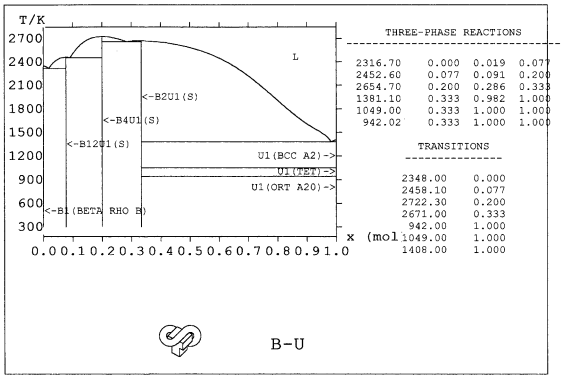

Fig. 14. Calculated B–U equilibrium phase diagram (this work) with quoted invariant or transition reactions.

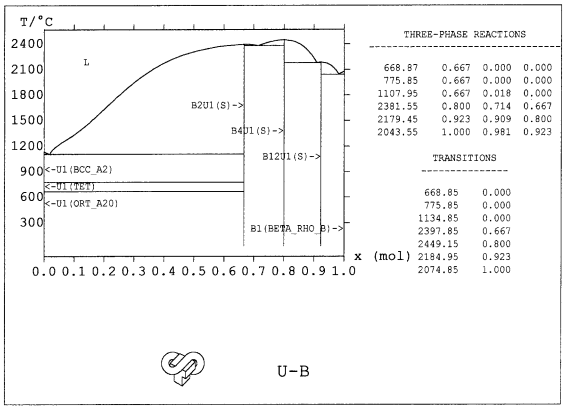

Fig. 15. Calculated B–U equilibrium phase diagram (this work) with different axes.

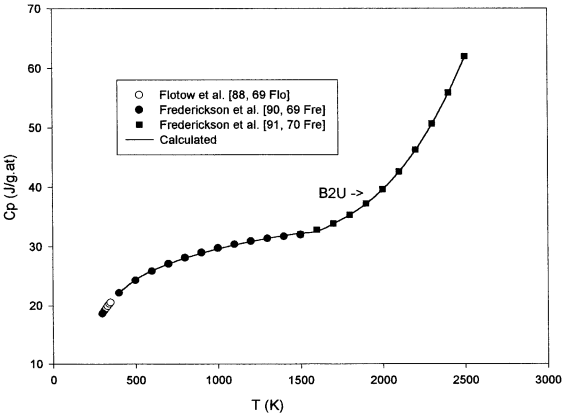

Fig. 16. Calculated heat capacity of the uranium diboride, UB_2, compared to the experimental information from various sources.

Fig. 17. Estimated heat capacity of the UB_4 and UB_{12} uranium borides compared to the experimental information from various sources.

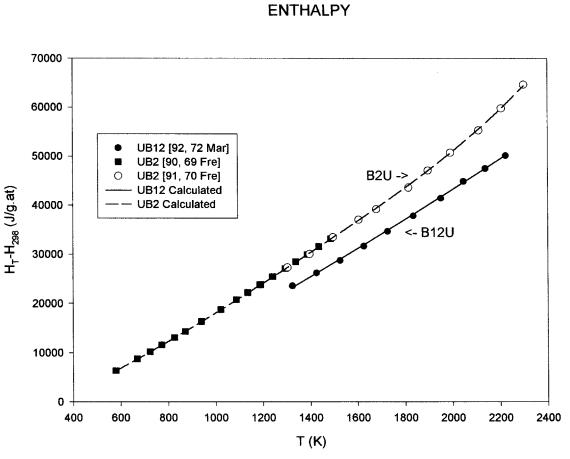

Fig. 18. Calculated heat content of the UB_{12} and UB_2 uranium borides compared to the experimental information from various sources.

Table 31
'Lattice-stabilities' or Gibbs energy parameters of elements

$G(\text{Sub}) - G(\text{Ref}) = a_k + b_k T + c_k T \log(T) + d_k T^2 + e_k T^3 + f_k T^{-1} + l_k T^{-2} + m_k T^{-3}$ (J/g at. for $T_k < T < T_{k+1}$)

Substance	Ref	T_k	a_k l_k	b_k m_k	c_k	d_k	e_k	f_k
SGTE lattice stabilities [6]								
B_1(L)	SER	298.15	40723.28	86.843839	−15.6641	-6.864515×10^{-3}	6.188775×10^{-7}	370843
		500	41119.70	82.101722	−14.982776	-7.095670×10^{-3}	5.073469×10^{-7}	335484
		2348	28842.01	200.94731	–31.4			
B_1(bet_rho_B)	SER	298.15	−7735.28	107.111864	−15.6641	-6.864515×10^{-3}	6.188775×10^{-7}	370843
		1100	−16649.47	184.801744	−26.6047	-7.980900×10^{-4}	-2.556017×10^{-8}	1748269
		2348	−36667.58	231.336244	−31.595753	-1.594880×10^{-3}	1.34719×10^{-7}	11205883
			3000	−21530.65	222.396264	−31.4		
C_1(gra_hex_A9)	SER	298.15	−17368.441	170.73	−24.3	-4.723×10^{-4}	0	2562600
			-2.643×10^{8}	1.2×10^{10}				
C_1(L)	SER	298.15	100000.559	146.10	−24.3	-4.723×10^{-4}	0	2562600
			-2.643×10^{8}	1.2×10^{10}				
U_1(ort_A20)	SER	298.15	−8407.734	130.95515	−26.9182	1.25156×10^{-3}	-4.42605×10^{-6}	38568
		955	−22521.8	292.121093	−48.66			
U_1(tet)	SER	298.15	−5156.136	106.976316	−22.841	-1.084475×10^{-2}	2.7889×10^{-8}	81944
		941.5	−14327.309	244.16802	−42.9278			
U_1(bcc_A2)	SER	298.15	−752.767	131.5381	−27.5152	-8.35595×10^{-3}	9.67907×10^{-7}	204611
		1049	−4698.365	202.685635	−38.2836			
U_1(L)	SER	298.15	3947.766	120.631251	−26.9182	1.25156×10^{-3}	-4.42605×10^{-6}	38568
		955	−10166.3	281.797193	−48.66			

Table 32
Gibbs energy parameters of condensed substances (elements and compounds)

$G(\mathrm{Sub}) - G(\mathrm{Ref}) = a_k + b_k T + c_k T \log(T) + d_k T^2 + e_k T^3 + f_k T^{-1} + l_k T^{-2} + m_k T^{-3}$ (J/g at. for $T_k < T < T_{k+1}$)

Substance	Ref	T_k	a_k l_k	b_k m_k	c_k	d_k	e_k	f_k
This work								
$U_1(\mathrm{fcc\_B1}, \delta)$	$U_1(\mathrm{bcc\_A2})$	298.15	+20000.00					
$U_1(\mathrm{bct}, \alpha)$	$U_1(\mathrm{bcc\_A2})$	298.15	20000.00					
$C_{0.500}U_{0.500}(\mathrm{fcc\_B1}, \delta)$	$C_1(\mathrm{gra\_hex\_A9})$ $U_1(\mathrm{bcc\_A2})$	298.15	−53413.24	35.39912	−5.457776	3.619306×10^{-3}	-0.5855×10^{-6}	−181089
$C_{0.500}U_{0.500}(\mathrm{bct}, \alpha)$	$C_{0.500}U_{0.500}(\mathrm{fcc\_B1}, \delta)$	298.15	500.00					
$C_{0.500}U_{0.500}(\mathrm{fcc\_B1}, \delta)$	SER	298.15	−58880.00	171.95288	−29.760578	0.057138×10^{-3}	-0.32422^{-6}	217780
$C_{0.667}U_{0.333}(\mathrm{fcc\_B1}, \delta)$	SER	298.15	6193.77 -8.81×10^6	−105.918145 4×10^8	7.8438233	$-1.0272821 \times 10^{-2}$	7.52067×10^{-9}	−5491740
$C_{0.667}U_{0.333}(\mathrm{bct}, \alpha)$	SER	298.15	−43704.05 -8.81×10^6	212.5905563 4×10^8	−34.9629114	8.537571×10^{-3}	-1.83221×10^{-6}	538235
$C_{0.600}U_{0.400}(\varepsilon)$	SER	298.15	−48891.92	175.15330	−30.012150	4.678713×10^{-3}	-1.36353×10^{-6}	288965
$B_{0.923}U_{0.077}(S)$	SER	298.15	−38367.06	121.772688	−18.189963	-4.829068×10^{-3}	0.26542×10^{-6}	413703
$B_{0.800}U_{0.200}(S)$	SER	298.15	−55835.03	129.114026	−20.213506	-5.578206×10^{-3}	0.35605×10^{-6}	371855
$B_{0.667}3U_{0.333}(S)$	SER	298.15 1600	−63972.50 −344980.46	137.55038 2063.58552	−22.286574 −283.582964	-5.157738×10^{-3} $106.066517 \times 10^{-3}$	0.39417×10^{-6} -8.73248×10^{-6}	310100 58632007

Table 33
Gibbs energy parameters of condensed solutions in the binary M–U systems (M = B, C)

$L[M_1, U_1]_1 = \Sigma_v L^v[M_1, U_1]_1 x_M x_U L^v[M_1, U_1]_1 = a^v[M_1, U_1]_1 + b^v[M_1, U_1]_1 T$ (J)

Phase	Formula	Excess interaction parameters	
		Name	
Liquid	$[C_1, U_1]_1\langle L\rangle$		
		$L^0[C_1, U_1]_1\langle L\rangle$	−247302.33
		$L^1[C_1, U_1]_1\langle L\rangle$	−109531.80
		$L^2[C_1, U_1]_1\langle L\rangle$	29843.99
		$L^3[C_1, U_1]_1\langle L\rangle$	29544.28
	$[B_1, U_1]_1\langle L\rangle$		
		$L^0[B_1, U_1]_1\langle L\rangle$	−87131.46
		$L^1[B_1, U_1]_1\langle L\rangle$	−45053.09
		$L^2[B_1, U_1]_1\langle L\rangle$	−63392.13
		$L^3[B_1, U_1]_1\langle L\rangle$	−58920.22
Fcc_B1, δ	$[C_1, C_2, Va]_1[U_1]_1\langle fcc\_B1, \delta\rangle$		
		$L^0[C_1, Va]_1[U_1]_1\langle fcc\_B1, \delta\rangle$	$87340.50 - 32.77837T$
		$L^0[C_1, C_2]_1[U_1]_1\langle fcc\_B1, \delta\rangle$	40264.38
		$L^1[C_1, C_2]_1[U_1]_1\langle fcc\_B1, \delta\rangle$	5013.70
		$L^2[C_1, C_2]_1[U_1]_1\langle fcc\_B1, \delta\rangle$	6965.85
Bct, α	$[C_1, C_2, Va]_1[U_1]_1\langle bct, \alpha\rangle$		
		$L^0[C_1, Va]_1[U_1]_1\langle bct, \alpha\rangle$	$87340.50 - 32.77837T$
		$L^0[C_1, C_2]_1[U_1]_1\langle bct, \alpha\rangle$	38923.11
		$L^1[C_1, C_2]_1[U_1]_1\langle bct, \alpha\rangle$	4222.04
		$L^2[C_1, C_2]_1[U_1]_1\langle bct, \alpha\rangle$	6965.85

Table 34
Assessed fundamental thermodynamic properties of stoichiometric compounds in the C–U and B–U binary systems

$C_p = C_k + D_k T + E_k T^2 + F_k T^{-2}$ ($C_k = -c_k; D_k = -2d_k; E_k = -6e_k; F_k = -2f_k$) (J/g at. K for $T_k < T < T_{k-1}$)

Compound	C_p (J/g at. K)	$\Delta H°_{f298.15}$ (J/g at.)	$S°_{298.15}$ (J/g at. K)
$C_{0.500}U_{0.500}$(fcc_B1, δ)	$29.760578 - 1.14276 \times 10^{-4}T + 1.945328 \times 10^{-6}T^2 - 435560T^{-2}$	−48534	29.874
$C_{0.665}U_{0.345}$(bct, α)	$35.330598 - 1.7696512 \times 10^{-2}T + 1.137234 \times 10^{-5}T^2 - 936860T^{-2}$	−30533	23.973
$C_{0.665}U_{0.345}$(fcc_B1, δ)	$-8.952231 + 2.122154 \times 10^{-2}T - 4.668 \times 10^{-8}T^2 + 11538952T^{-2}$		
$C_{0.600}U_{0.400}$(ε)	$30.012150 - 9.357426 \times 10^{-3}T + 8.18118 \times 10^{-6}T^2 - 577930T^{-2}$	−38349	26.680
$B_{0.923}U_{0.077}(S)$	$18.189963 + 9.658136 \times 10^{-3}T - 1.59252 \times 10^{-6}T^2 - 827406T^{-2}$	−29753	7.5191
$B_{0.667}U_{0.333}(S)$	$22.286574 + 1.0315476 \times 10^{-2}T - 2.36502 \times 10^{-6}T^2 - 620200T^{-2}$	−54810	18.175
($T > 1600$)	$283.582964 - 2.12133034 \times 10^{-1}T + 5.239488 \times 10^{-5}T^2 + 117264014T^{-2}$		
$B_{0.800}U_{0.200}(S)$	$20.213506 + 1.1156412 \times 10^{-2}T - 2.1363 \times 10^{-6}T^2 - 743710T^{-2}$	−46837	13.682

Appendix A

See Table 31.

Appendix B

See Table 32.

Appendix C

See Table 33.

Appendix D

See Table 34.

References

[1] P.Y. Chevalier, E. Fischer, B. Cheynet, A. Rivet, G. Cenerino, in: Proceedings of the International Conference on the Thermodynamics of Alloys, Marseille, France, 2–5 September 1996, J. Chim. Phys. 94 (1997) 849.
[2] P.Y. Chevalier, E. Fischer, J. Nucl. Mater. 257 (1998) 213.
[3] P.Y. Chevalier, E. Fischer, B. Cheynet, private communication, 2000.
[4] P.Y. Chevalier, E. Fischer, B. Cheynet, Int. Conf. Calphad XXVIII, Grenoble, May 1997.
[5] K. Hack (Ed.), The SGTE Casebook, Thermodynamics at Work, Materials Modelling Series, Institute of Materials, 1996.
[6] A.T. Dinsdale, Calphad 15 (4) (1991) 317.
[7] H.L. Lukas, E.Th. Henig, B. Zimmermann, Calphad 1 (3) (1977) 225.
[8] M. Hansen, K. Anderko, Constitution of Binary Alloys, McGraw-Hill, New York, 1958.
[9] R.P. Elliott, Constitution of Binary Alloys, First Supplement, McGraw-Hill, New York, 1965.
[10] F.A. Shunk, Constitution of Binary Alloys, Second Supplement, McGraw-Hill, New York, 1969.
[11] R. Hultgren, P.D. Desai, D.T. Hawtkins, M. Gleiser, K.K. Kelley, Selected Values of the Thermodynamic Properties of Binary Alloys, American Society of Metals, Metals Park, OH, 1973.
[12] E.K. Storms, A Critical Review Academic Publishers, The Refractory Carbides, vol. 171–213, 1967.
[13] T.B. Massalski, ASM'S Binary Alloy Phase Diagrams, second ed., 1990.
[14] R. Benz, C.G. Hoffman, G.N. Rupert, High Temp. Sci. 1 (1969) 342.
[15] R.E. Rundle, N.C. Baenziger, A.S. Wilson, R.A. McDonald, J. Am. Chem. Soc. 70 (1948) 99.
[16] L.M. Litz, A.B. Garrett, F.C. Croxton, J. Am. Chem. Soc. 70 (1948) 1718.
[17] W. Mallet, A.F. Gerds, D.A. Vaughan, J. Electrochem. Soc. 98 (1951) 505.
[18] I. Higashi, Rikagaku Kenkyusho Hokoku 37 (1961) 271.
[19] A.E. Austin, Acta Crystallogr. 12 (1959) 159.
[20] M. Atoji, R.C. Medrud, J. Phys. Chem. 31 (1959) 332.
[21] R. Chang, Acta Crystallogr. 14 (1961) 1097.
[22] T. Kikido, US At. Energy Commun. TID-7603 (1960) 107.
[23] M.A. Bredig, J. Am. Ceram. Soc. 43 (1960) 493.
[24] W.B. Wilson, J. Am. Ceram. Soc. 43 (1960) 77.
[25] P. Magnier, A. Accary, in: L.E. Russel et al. (Eds.), Carbides in Nuclear Energy, vol. 1, Macmillan, London, 1964, p. 22.
[26] F. Anselin, G. Dean, R. Lorenzelli, R. Pascard, in: L.E. Russel et al. (Eds.), Carbides in Nuclear Energy, vol. 1, Macmillan, 1964, p. 113.
[27] S.C. Carniglia, in: L.E. Russel et al. (Eds.), Carbides in Nuclear Energy, vol. 1, Macmillan, London, 1964, p. 403.
[28] P. Magnier, J. Trouvé, A. Accary, in: L.E. Russel et al. (Eds.), Carbides in Nuclear Energy, vol. 1, Macmillan, London, 1964, p. 95.
[29] W.G. Witteman, M.G. Bowman, quoted by E.K. Storms, US At. Energy Comm. LA-2942, 1964, 254pp; US At. Energy Commun. TID-7676 (Fourth Uranium Carbide Meeting, East Hartford, Conn.) 1963, 121.
[30] W. Mallet, A.F. Gerds, H.R. Nelson, J. Electrochem. Soc. 98 (1952) 505.
[31] B. Blumenthal, J. Nucl. Mater. 2 (3) (1960) 197; ANL-6099 (1959) 72; TID-7523, pt. 1, 1956, p. 65.
[32] T.H. Carter, Report CT 609 (1943) (USAEC. Technical Information Services, Washington, DC).
[33] A.I. Snow, Reports CT 954 (1943) and CT 1102 (1943) (USAEC. Technical Information Services, Washington, DC).
[34] P. Chiotti, J. Am. Ceram. Soc. 35 (1952) 123.
[35] L.D. Brownlee, J. Br. Nucl. Energy Conf. 4 (1959) 35.
[36] H.W. Newkirk Jr., J.L. Bates, US At. Energy Comm. HW-59468, 1959, 5pp.
[37] W.G. Witteman, J.M. Leitnaker, M.G. Bowman, US At. Energy Comm. TID 7603 (1961) 48.
[38] G.D. White, P.D. Shalek, J.T. Dusek, US At. Energy Comm. ANL 6868 (1963) 152.
[39] W. Chubb, W.M. Phillips, Trans. ASM 53 (1961) 465.
[40] W.B. Wilson, J. Am. Ceram. Soc. 43 (2) (1960) 77.
[41] P. Guinet, H. Vaugoyeau, P.L. Blum, C. R. Acad. Sci. Paris t.261 (2 août 1965), Groupe 7, p. 1312.
[42] M.B. Sears, L.M. Ferris, R.J. Gray, J. Electrochem. Soc. 113 (3) (1966) 269.
[43] M. Tetenbaum, P.D. Hunt, J. Nucl. Mater. 40 (1971) 104.
[44] H. Tagawa, K. Fujii, J. Nucl. Mater. 39 (1971) 109.
[45] T. Kurasawa, H. Watanabe, T. Kikuchi, J. Nucl. Mater. 43 (1972) 192.
[46] F.H. Schneider, A. Naoumidis, H. Nickel, J. Nucl. Mater. 43 (1972) 175.
[47] H.L. Scherff, A. Springer, J. Nucl. Mater. 56 (1975) 153.
[48] M.D. Burdick, H.S. Parker, R.S. Roth, E.L. McGandy, J. Res. Nat. Bur. Stand. 54 (1955) 217.
[49] F.A. Rough, Nuclear Fuels Newsletter, WASH-702, E. Epremian (Ed.) Tech. Inform. Ser. Extension, Oak Ridge, Tenn., May 1957.
[50] A.C. Secrest, E.L. Foster, R.F. Dickerson, Preparation and Properties of Uranium Monocarbide Castings, BMI-1309, Battelle Memorial Inst., Columbus 1, OH, 1959.
[51] M.B. Sears, L.M. Ferris, R.J. Gray, J. Electrochem. Soc. 113 (1966) 269.

[52] J.D. Farr, E.J. Huber Jr., E.L. Head, C.E. Holley Jr., J. Phys. Chem. 63 (1959) 1455.
[53] J.W. Droege, A.W. Lemmon Jr., R.B. Filbert Jr., Batelle Mem. Inst. Rept. BMI-1313, 38 and A-5, 1959.
[54] C.B. Alcock, P. Grieveson, Thermodynamics of Nuclear Materials, IAEA, Vienna, 1962, p. 563.
[55] P.A. Vozella, A.D. Miller, M.A. Decrescente, Pratt and Whitney Aircraft Corp. Rept. CNLM-5619, 1964.
[56] W.C. Robinson Jr., P. Chiottu, Ames Lab., Iowa State Univ. of Sci. and Tech., Contract W-7405-enf. 82, 1964.
[57] E.K. Storms, Los Alamos Sci. Lab. Rept. LA-DC-6953, 1965.
[58] F. Benesovsky, E. Rudy, Planseeber. Pulvermetll. 9 (1961) 65.
[59] S. Fujishiro, J. At. Energy Soc. Jpn. 3 (1961) 913.
[60] J.R. Piazza, M.J. Sinnott, J. Chem. Eng. Data 7 (1962) 451.
[61] H.K. Lonsdale, J.N. Graves, Thermodynamics of Nuclear Materials, IAEA, Vienna, 1962, p. 601.
[62] J.M. Leitnaker, W.G. Witteman, J. Chem. Phys. 36 (1962) 1445.
[63] H. Eich, E.J. Rauh, R.J. Thorn, Thermodynamics of Nuclear Materials, IAEA, Vienna, 1962, p. 549.
[64] E.J. Huber Jr., E.L. Head, C.E. Holley Jr., J. Phys. Chem. 67 (1963) 1730.
[65] J.H. Norman, P. Winchell, J. Phys. Chem. 68 (1964) 3802.
[66] W.K. Behl, J.J. Egan, J. Electrochem. Soc. 113 (4) (1966) 376.
[67] L.S. Levinson, J. Chem. Phys. 38 (9) (1963) 2105.
[68] J.B. Moser, O.L. Kruger, J. Appl. Phys. 38 (8) (1967) 3215.
[69] J.M. Leitnaker, T.G. Godfrey, J. Nucl. Mater. 21 (1967) 175.
[70] J.A. Craig, R.E. Balzhiser, D.V. Ragone, Trans. Metall. Soc. AIME 242 (1968) 1809.
[71] A.C. MacLeod, J. Inorg. Nucl. Chem. 31 (1969) 715.
[72] C. Affortit, J. Nucl. Mater. 34 (1970) 105.
[73] V.V. Akhachinski, S.N. Bashlykov, At. Energy 29 (6) (1970) 439.
[74] F.L. Oetting, J.D. Navratil, E.K. Storms, J. Nucl. Mater. 45 (1972/1973) 271.
[75] M. Hoch, E.F. Juenke, L.H. Sjodahl, Thermodynamics of Nuclear Materials, Vienna, 1967, IAEA, Vienna, 1968, p. 497.
[76] S.S. Nikol'skii, High Temp. 7 (5) (1969) 873 (translated from Teplofiz. Vysok. Temp.).
[77] S.S. Nikol'skii, I.N. Levina, High Temp. 7 (6) (1969) 1087 (translated from Teplofiz. Vysok. Temp.).
[78] G.E. Murch, R.J. Thorn, Philos. Mag. 34 (2) (1976) 299.
[79] R.B. McLellan, J. Phys. Chem. Solids 40 (1979) 311.
[80] R.B. McLellan, J. Phys. Chem. Solids 41 (1980) 412.
[81] L. Brewer, D.L. Sawyer, D.H. Templeton, C.H. Dauben, J. Am. Ceram. Soc. 34 (1951) 173.
[82] F. Bertaud, P. Blum, C. R. 229 (1949) 666.
[83] P. Blum, F. Bertaud, Acta Crystallogr. 7 (1954) 81.
[84] B.W. Howlett, J. Inst. Met. 88 (1959–1960) 91.
[85] H.J. Eding, E.M. Carr, US At. Energy Comm. ANL-6339, 1961, 20.
[86] R.W. Mar, J. Am. Ceram. Soc. 58 (3–4) (1975) 145.
[87] L.G. Podobeda, V.A. Malykh, Colloque Thermodynamique Mat. Nucl., Vienne, 4–8 September 1967, SM 98/51.
[88] H.E. Flotow, D.W. Osborne, P.A.G. O'Hare, J.L. Settle, F.C. Mrazek, W.N. Hubbard, J. Chem. Phys. 51 (2) (1969) 583.
[89] C. Alcock, P. Grieveson, Thermodynamics of Nuclear Materials, IAEA, Vienna, 1962, p. 563.
[90] D.R. Fredrickson, R.D. Barnes, M.G. Chasanov, R.L. Nuttall, R. Kleb, W.N. Hubbard, High Temp. Sci. 1 (1969) 373.
[91] D.R. Fredrickson, R.D. Barnes, M.G. Chasanov, High Temp. Sci. 2 (1970) 299.
[92] R.W. Mar, N.D. Stout, J. Chem. Phys. 57 (12) (1972) 5342.
[93] M.S. Borovikova, V.V. Fesenko, J. Less-Common Met. 117 (1986) 287.
[94] R. Chipaux, G. Cecilia, M. Beauvy, R. Troc, J. Less-Common Met. 121 (1986) 347.
[95] O.H. Krikorian, Rap. UCRL-51043, 1971; reported in [80, 86Chi].
[96] P.E. Potter, Gmelin Handbook of Inorganic Chemistry, Boron Supplement, vol. 2, Springer, Berlin, 1981.
[97] THERMALLOY solution database, THERMODATA, BP 66, 1001, avenue Centrale, 38402 St Martin d'Hères cedex, France.